

Optimal Utilization of Multiple Stored Media in Flexible Storage Facilities: An Application in Intermittent Electricity Production Using Salt Caverns

Xavier Etienne Roger de Graaf¹ and Reinhard Madlener^{2,*}

¹ RWTH Aachen University, Templergraben 55, 52056 Aachen, Germany

² Institute for Future Energy Consumer Needs and Behavior (FCN), School of Business and Economics /
E.ON Energy Research Center, MathieustraÙe 10, 52074 Aachen, Germany

November 2015

Abstract

Intermittent electricity production due to increasing shares of renewable energies, carbon capture and storage technologies to retard climate change and the increasing usage of hydrogen for transport applications have one thing in common: They all need long-term large-scale storage facilities. Consequently, a future competition for the most cost-efficient storage sites is likely. This study describes an economic storage model which enables the user to identify the most economic utilization of one specific cavern storage site. Salt caverns represent the most flexible large-scale geological storage. Currently, salt caverns are mainly in use as seasonal gas storage. Europe offers a high potential for further cavern storage use. The model includes technical properties of salt caverns as storage facilities, and hydrogen, compressed air, methane and carbon dioxide as storage media. Real options analysis is used to value the stored medium during the lifetime of the cavern storage. The model suggests, based on the expected market development, the most attractive storage medium to maximize the overall discounted earnings. Potential storage costs for each application are compared with economic gains or cost savings (e.g. avoided carbon tax, revenues from peak-load sale of electricity, etc.) which are generated by an optimal time-dependent usage of the stored medium. As the simulation results will show, the estimated storage costs both for the natural gas storage as well as the CAES exceed the discounted revenues in the base variant. On top of that, the value of intertemporal arbitrage of carbon dioxide is not enough to cover the marginal costs.

Keywords: Energy storage, CAES, stochastic modelling, seasonality, Markov regime switching, real options

* Corresponding author. Tel. +49 241 80 49 820, RMadlener@eonerc.rwth-aachen.de (R. Madlener).

Nomenclature

Symbol	Description
RE	Renewable energies
EEX	European Energy Exchange
OTC	Over-the-counter
EEG	Renewable energy law
CAES	Compressed air energy storage
EUA	European Emission Allowance

1. Introduction

Intermittent electricity production due to increasing shares of renewable energies (RE), carbon capture and storage technologies to mitigate climate change, and the increasing usage of hydrogen for transport applications have one thing in common: They all need long-term large-scale storage facilities. Consequently, a future competition for the most cost-efficient storage sites is likely. The topic of this study is unique in multiple dimensions. Firstly, academic literature which gives a direct economic comparison of different usage scenarios of one specific cavern storage does not exist. Secondly, so far, the possibility to switch from one usage scenario to a second usage scenario during the economic lifetime of a cavern storage has not been studied. Consequently, this study gives a new perspective on the valuation of geological cavern storages. Instead of researching the most suitable storage type for a certain medium, the following study identifies the most economic utilization in terms of storage medium of one specific cavern storage.

To model the most economic utilization of the storage units, several assumptions on the market development and prices of electricity, natural gas and carbon dioxide are made. Based on the assumptions, complex price models for electricity, gas and carbon dioxide are developed to capture the stochastic price movements over the following 25 years.

An increasing share of renewable energies (RE) in the European and especially German electricity production leads to increasing volatility in electricity supply. Since electricity demand and supply have to be in balance at every moment in time and electricity is nearly a non-storable commodity, challenging requirements for future expansion of the electricity grid to avoid blackouts are in place. One part of the solution is the construction of large-scale electricity storages that enables to flatten the volatility of electricity supply. This will cause an increasing need for suitable storage sites.

Not only the electricity market but also the gas market will need more storage capacity in the future. This is due to the fact that the share of long-distance imports of natural gas is in-

creasing, since national and European natural gas fields are reaching depletion. At the same time, the overall natural gas consumption is expected to stagnate as in recent years (Petroleum, 2015) or increase due to the growing usage of flexible, less carbon dioxide intensive, gas-fired power plants. This in turn leads to an increasing need for large-scale gas storage sites to balance fluctuating consumption and prices.

The plan of the European Union is to reduce its carbon dioxide emissions by 80-95% until 2050¹ (bpb, 2013; CCC, 2015). To reach this ambitious goal, the vast majority of all fossil fuel powered power plants will be substituted by RE. Moreover, technologies to capture and use the excessive amounts of carbon dioxide are needed (Fischedick, Esken, Luhmann, Schüwer, & Supersberger, 2007). This is why large-scale intermediate or long-term carbon dioxide storage facilities will be needed in the upcoming 35 years.

The expected developments outlined above can lead to a situation in which different storage media compete for the same storage site. Most likely, salt cavern storage sites are the type of sites which will be suitable for all applications mentioned above. Salt caverns represent the most flexible large-scale geological storage option. Currently, they are mainly in use as seasonal gas storage. These sites are very suitable for compressed air storages, too. Europe offers a high potential for further cavern storage expansion (section 5).

The following sections describe how a simple storage model can be used to answer the question which storage medium is, from an economic perspective, most suitable to store in a large-scale salt cavern. The model includes technical properties of salt caverns as storage facilities, and hydrogen, compressed air, methane and carbon dioxide as storage media.

Potential storage costs for each application are compared with economic gains or cost savings (e.g. avoided carbon tax, revenues from peak-load sale of electricity, etc.) which are generated by an optimal time-dependent usage of the stored medium.

The remainder of this paper is organized as follows. Section 2 gives an overview of related literature in the field of study and summarizes the most important theoretical foundations for this study. Further, the datasets for the simulation are introduced. Section 3 analyses the status quo and expected development on the electricity, natural gas, hydrogen and emission allowances market. The findings are used in section 4 to explain the existence of certain price patterns. In section 4, we introduce the most suitable prices modelling approach, describe the developed price models for each storage medium, and present the simulation results. Section 5 describes the technical and economic properties of salt cavern storages in general and specifically for a selected site. After an analysis of already existing and potential sites the de-

¹ Based on 1990 emission levels

scription of the working principle of a salt cavern is given. Moreover, the technical restrictions of each storage medium and the cost associated with the usage of a certain medium are outlined in section 5 as well. At last, an assumption on the cost for the development of a new gas cavern storage is performed. Section 6 presents the general storage model with an analysis of all assumptions which have been made in order to make the storage model solvable in a reasonable time span. Also, different scenarios for the usage of the storage are explained and incorporated in the storage model. Finally, section 7 contains the presentation and analysis of the storage model results. A sensitivity analysis shows the most influential factors on the economics of the storage operation. Section 8 concludes. The simulation results show that the estimated storage costs both for the natural gas storage as well as the CAES exceed the discounted revenues in the base variant. Besides, the value of intertemporal arbitrage of carbon dioxide is insufficient to cover the marginal costs.

2. Theoretical foundation

The theoretical background of our study is based on three fundamental bases. Firstly, through a Monte Carlo simulation several price paths are simulated and the value of the storage is estimated for each price paths separately. On top of that, the decision of the storage operator can be modelled as a real option, with a decision at each time step to inject or withdraw. This treatment corresponds to the Real Options Theory, which is described below. Secondly, popular theoretical approaches to forecast electricity prices are described with an analysis of benefits and downsides of each approach. Thirdly, a brief theoretical introduction into different approaches of storage valuation is given in the last part of this section.

2.1 Real Options Theory

Dixit (1989) describes the real options theory as an approach which integrates the valuation of sunk costs for entry and exit decisions ('uncertainty hysteresis') in an investment decision. Company A, for instance, needs an initial investment sum k to become active to produce output at a variable cost w . The company A can decide to discontinue operations but has to pay a lump-sum cost l to do so (Dixit, 1989). To re-continue operations it has to pay entry cost k again. On top of that, the firm's discount rate for the initial investment costs is p . The uncertainty to enter or to exit the market arises from the non-constant market price. If the price fluctuations are expected to be mean-reverting and the price is just at the level $w + pk$, with equal probabilities of a price change up or down at each point in time, the investment opportunity will yield a net present value of zero. If the company waits until the next period and the price has gone up, an investment will yield a positive expected present value. Consequently,

the investment decision can be seen as an option, which has a value of waiting. This option will only be exercised if the option is in the money ($\text{price} > w + pk$) (Dixit, 1989).

In a nutshell, the main idea of the real options theory is to consider sequential, irreversible investments under uncertainty as a purchase of a real option, which allows firms to postpone full commitment until a significant part of the uncertainty has been resolved. The option is only exercised if the investment yields a positive net present value (Adner & Levinthal, 2004).

2.2 Price simulation

The article by Rafał Weron, Bierbrauer, and Trück (2004) can be seen as one of the first papers which focuses on the simulation of electricity spot prices with a jump diffusion and a regime switching model including deseasonalization. It was followed and refined in later papers of Weron. In 2013, Janczura, Trück, Weron, and Wolff (2013) performed an extensive study on different methods of spike identification and deseasonalization of electricity spot price data. The findings are used in this paper for deseasonalization, outlier filtering as well as the Markov regime switching approach.

Muche (2009) shows very descriptive the entire spot price simulation process with a deterministic price component with a stochastic jump process. His work is partly based on Weron's findings. Muche neglects negative prices to achieve a simpler price model. Keles, Genoese, Möst, and Fichtner (2012) incorporate negative prices and compare different modified statistical and reduced form models to simulate electricity spot prices. The detailed decomposition of historical prices using a deterministic and stochastic component will be used in this paper.

Weron (2007) gives a good overview of different classes of modelling approaches for electricity markets. Recently, Rafał Weron (2014) published an extensive literature review on different approaches for electricity price forecasting. The most important findings will be presented below. Electricity spot price modeling approaches can be categorized into five types:

- (1) **Multi-agent models**, which represent the price process by matching the demand and supply of interacting heterogeneous agents (utility companies).
- (2) **Fundamental models**, which determine the price path by modeling impacts of important economic and physical factors on the price of electricity.
- (3) **Reduced-form models** analyze and describe the statistical properties of electricity in an econometrical model over time.
- (4) **Statistical approaches** are either directly applied statistical techniques of load forecasting or econometric models adapted to the power market.

(5) **Computational intelligence techniques** combine ‘nature-like’ processes such as learning, evolution and fuzziness to create models which are able to adapt to complex dynamic systems.

In practice, many applied modeling and price forecasting approaches are hybrid solutions based on two or more techniques (Rafał Weron, 2014). In this paper we will focus, just as most related literature, on reduced form modeling approaches. We elaborate on different type of reduced-form models below.

Reduced-form models

Reduced-form models offer the best of two worlds by managing a trade-off between model parsimony and adequacy to capture the unique characteristics (sharp spikes and drops) of electricity prices (Rafał Weron, 2014). Frequently used price models are one-factor stochastic models with a time-dependent drift $\mu(t)$ (Boogert & De Jong, 2008; Schwartz, 1997). These approaches use a diffusion-type stochastic differential equation (Rafał Weron et al., 2004). The model shown below consists of a mean-reverting component κ and a drift term $\mu(t)$.

$$\frac{dP(t)}{P(t)} = \kappa[\mu(t) - \ln P(t)]dt + \sigma dW(t) \quad (1)$$

$dW(t)$ describes a Wiener process (Brownian Motion)

The mean reversion model proposed above does not account for the “jumpy” character of electricity price movements, which is why Felix, Woll, and Weber (2013), Thompson, Davison, and Rasmussen (2009), Holland (2008) and Rafał Weron et al. (2004), among others, use an extension of equation (1) and include a jump diffusion process based on a Poisson process, which gives a *Jump-diffusion model*:

$$dP(t) = \kappa \mu(t)dt + \sigma dW(t) + J_t dq_t \quad (2)$$

Seifert and Uhrig-Homburg (2007) find that Poisson jump and Poisson spike processes with constant intensities perform rather poor for the German EEX spot price estimation. The usage of stochastic jump intensity reduces these problems.

The advantage of *Markov regime-switching models* over *jump-diffusion models* is the fact that *Markov regime-switching (MRS) models* can exhibit spike clustering on the daily time scale as well as the hourly time scale in a very natural way (Rafał Weron et al., 2004). An unobservable variable in the time series will trigger a switch between a predefined number of regimes. MRS models are very flexible and allow mean reversion (temporary dependence within the regimes). Each regime can have an independent stochastic price process (Carmona & Ludkovski, 2010; Keles, Genoese, et al., 2012; Rafał Weron et al., 2004) or can be modelled identically (mostly mean-reverting). Fanone, Gamba, and Prokopczuk (2013) proposed

two independent Lévy processes, the first one describes the fluctuations around the long-term mean while the second Lévy process models the strong spikes and drops.

Another approach is to include different regimes in the same price process (Bierbrauer, Trück, & Weron, 2004; Carmona & Ludkovski, 2010; Z. Chen & Forsyth, 2010; Rafał Weron et al., 2004). The base regime is typically modelled by a mean-reverting diffusion (Huisman, Hurman, & Mahieu, 2007). Janczura et al. (2013) use a structure based on three regimes for deseasonalized spot prices. The base regime ($R_t=1$) describes the regular price movement based on a mean-reverting, heteroscedastic process (Janczura et al., 2013; Janczura & Weron, 2012):

$$dX_{t,1} = (\alpha_1 - \beta_1 X_{t,1})dt + \sigma_1 |X_t|^\gamma dW_t \quad (3)$$

The second regime ($R_t=2$) describes price spikes caused by unexpected demand peaks or supply shortages and can be modelled as lognormal, Gaussian, Pareto, Weibull or exponential distributed spike regime. A shifted log-normal distribution, as described in Janczura et al. (2013), with q_2 as third quantile is stated below:

$$\log(X_{t,2} - q_2) \sim N(\mu_2, \sigma_2), \quad X_{t,2} > q_2 \quad (4)$$

The third regime ($R_t=3$) describes sudden price drops, modelled according to the shifted ‘inverse log-normal’ law with q_3 as the first quartile of the dataset (Janczura et al., 2013):

$$\log(-X_{t,3} + q_3) \sim N(\mu_3, \sigma_3), \quad X_{t,3} < q_3 \quad (5)$$

An optimized algorithm with three or two regimes of the MRS is proposed by Janczura and Weron (2012) in order to estimate the parameters of the MRS with significantly lower computational burden.

As described by Rafał Weron (2014), the results of the MRS are conflicting. Kosater and Mosler (2006) reach satisfying results for the medium term price forecasting of the EEX spot prices, while Liebl (2013) observes a poor performance of the MRS model compared to three factor models. All in all, a hybrid model consisting of a MRS model to model the especially spiky prices of the EEX spot price market and a similar day method to describe a recurring pattern could yield a reasonable performance compared to the other possible approaches mentioned above (Rafał Weron, 2014)

2.3 Storage valuation

There are four popular theoretical approaches to capture not only the intrinsic value (predictable seasonal pattern) but also the extrinsic value (reaction on price fluctuations) on a spot-based storage strategy. The first three approaches are mathematical sophisticated models which are developed to increase computation speed and overcome some limitations, while the fourth approach implies rather simplistic linear programs and heuristics of practitioners.

The *stochastic control approach* is used by Thompson et al. (2009) and Weston and Ronn (2002), among others. The models are based on Bellman equations, connecting directly the stochastic price process with the optimal storage strategy. These equations are solved through numerical partial differential equation techniques (PDE) (Thompson et al., 2009). The paper was originally written in 2003 and was the first paper to value gas storages with PIDEs. Through clever mathematical simplifications, the resulting equation turns out to be simple. However, a change in price processes can violate some mathematical simplifications. Based on the approach of Thompson et al. (2009), Felix et al. (2013) assess the value of a gas storage and limited market liquidity. We incorporated the storage data from that paper in chapter 5. Carmona and Ludkovski (2010) solve the *stochastic control approach* with a probabilistic solution based on optimal multiple stopping problems. This approach decreases the limitations in terms of price models and storage constraints experienced with PDE techniques. However, resulting the algorithm has the length of multiple pages and is not easily adjustable, due to several mathematical simplifications and assumptions (Carmona & Ludkovski, 2010). Z. Chen and Forsyth (2010) integrate an one-factor, two-regime Markov regime switching approach in the *stochastic control approach* and solve the resulting PDEs with a semi-Lagrangian time-stepping scheme. The result is not only mathematically complex but also numerically difficult to trace and to achieve convergence.

The second approach, the *Monte Carlo approach*, separates the stochastic price process from the optimal strategy estimation. This is an advantage since it makes the integration of more detailed price processes easier. Moreover, it simplifies the integration of additional operation constraints. The major drawback of the Monte Carlo approach is the rather long computation time (Boogert & De Jong, 2008).

The storage can be seen as an American option, because the storage operator is faced with a timing problem when to inject and withdraw. An American option can be exercised in every moment of time till the expiry date. The option holder has to decide when to exercise the option (Boogert & De Jong, 2008). Longstaff and Schwartz (2001) introduced the Least Squares Monte Carlo method to solve American option pricing by simulation. This approach has become quite popular, which is why Boogert and De Jong (2008) uses this approach to estimate the storage value by means of dynamic programming.

A third, rather new approach is the *approximate linear programming*, to solve intractable Markov Decision Processes (MDPs). The main idea is to use approximate linear programming to make high dimensional price models, which are often untraceable in stochastic dynamic programming, solvable within an expectable computation time (Lai, Margot, & Secomandi, 2010). The approach of Nadarajah, Margot, and Secomandi (2014) is based on

findings by Lai et al. (2010) and extended with a Markov Decision Process as price model. Nadarajah et al. (2014) describes this approach for a gas storage valuation based on a forward curve price estimation. This approach is mathematically rather challenging especially with price models exceeding a one-factor model and not easily extendible with additional storage constraints. This approach could be used in further research as model for this paper.

A fourth, rather simplistic approach, is heavily used by practitioners: The *heuristic approach*. Heuristic approaches use multi-factor price models, which can incorporate the real price movements more sophisticated. The high dimensionality rules out the application of dynamic programming approaches (Thompson, 2012). Heuristic approaches generate n different price paths (often hundreds or thousands). Each price path contains t time steps. At each time step a decision has to be made to buy or sell (inject / withdraw) under the assumption that future prices are not affected by the decision. The final value is defined as the average value of all the discounted valuation outcomes of all price paths. The heuristic approaches use often linear programs in combination with Monte Carlo simulations (Lai et al., 2010). Heuristic approaches have shown to result in nearly optimal injection and withdrawal strategies but with the drawback of high computational complexity (Lai et al., 2010; Thompson, 2012).

Holland (2008) formulates a very basic MILP (mixed integer linear program) to allow energy traders to measure their impact on the storage valuation by their trading decisions on a daily basis. By contrast, Muche (2009) uses the day-ahead spot prices to plan an intra-day unit commitment. Keles, Hartel, Möst, and Fichtner (2012) and Drury, Denholm, and Sioshansi (2011) use mixed integer linear programs (MILP) and linear programs (LP), respectively to value a CAES. The rather simplistic approaches yield reliable results (Drury et al., 2011). Keles, Hartel et al. (2012) propose a simplistic mixed linear program to model a CAES properly. The authors assume gas and CO₂ prices to be static, and the overall optimization is only conducted over 365 days with a perfect foresight on price over the entire timeframe. The basic structure of this model will be used in this paper. Sioshansi et al. (2009) estimates the value of electricity storage based on arbitrage without specifying an exact storage. The paper gives a good overview of the most economic storage size and assumable arbitrage revenues. Most importantly, Sioshansi et al. (2009) study the impact of perfect and imperfect foresight on prices on the storage valuation. These findings will be used in our model as data and for comparison. Conolly et al. (2011) research optimal operation strategies of pumped hydro storage based on spot price spreads with a simple linear program. The basic structure of this linear program can be seen as basis for this paper. The most valuable outcome is the study of valuation differences between perfect foresight and limited foresight on future prices.

2.4 CAES model

Gatzen (2008) developed a CAES model based on a mixed linear program. Loisel et al. (2010) refined this model with technical preferences and extended it with assumptions on the reserve power market. The integration of the reserve power market as additional revenue stream for the CAES can be included to extend this paper. Drury et al. (2011) find that CAES revenues solely based on electricity arbitrage are unlikely to support investment in most market locations, but with additional revenues from the reserve market, the investment can be economic in several markets. The technical properties of the CAES as well as the cost estimations and CAES model formulation are used as basis in this paper.

2.5 Data used

Table 1 gives a brief review of the used datasets for price simulation purpose. Especially the datasets of natural gas and EUA are rather short, due to the very recent establishment of those spot markets. The spot market for electricity (EPEXSPOT) reaches back to the liberalization of electricity markets in the early 2000s. The liquidity on the day-ahead hourly spot market increased steadily and can be seen as very liquid from 2005 on. In order to account for the impact of the increasing share of RE on the volatility and price drops the selected data set starts in 2009. The limited calibration time period (max. six years for electricity) compared to the simulation time of 25 years, can influence the identified patterns in section 4. Consequently, the simulated price paths should be seen as one potential future outcome.

Table 1: Description of datasets used for price simulation

No.	Name	Period	No. of values	Source	Comments
1	Natural gas spot market daily reference price – NCG hub	31 May 2011 – 21 Sep 2015	1575	(EEX, 2015c)	NCG gas spot market daily reference price was established in May 2011 by the EEX. Due to higher liquidity in the NCG market area in the first two years, prices from the NCG area are used. The price is determined every day. Hourly trading is possible but trading volume is very volatile and consequently the market price can only be determined for a few hours per day.
2	EPEXSPOT day-ahead hour-	01 Jan 2009 – 02 Sep 2015	58464	(EEX, 2015a)	Data from Phelix day-ahead hourly electricity spot market. Each day at

	ly spot prices (Phelix)				noon the hourly prices for the next day are determined and contracts settled. Market is very liquid, price range from -500 €/MWh – 3,000 €/MWh possible.
3	EPEXSPOT Day-ahead Daily spot prices (Phelix)	01 Jan 2009 – 02 Sep 2015	2436	(EEX, 2015d)	Data from Phelix day-ahead base-load contract. The contract is traded daily and contains of a 24h delivery of electricity. Prices are determined each day at noon. Base-load price-path are used for the estimation of long-term cycles.
4	EEX emission market (secondary)	01 Jan 2013 – 21 Sep 2015	994 (686)	(EEX, 2015b)	EUA data from secondary market transactions. EEX EUA emission spot market exists from Jan 2013 on. Only traded on weekdays and liquidity is in 2013 rather poor. To complete the dataset missing data points filled with moving average of surrounding market prices. Primary market is a EUA auction with far less yearly trading days.

3 Storage media – market development

The following subsections give a brief summary of market developments in the electricity, natural gas, carbon dioxide and hydrogen markets in recent years. The four different storage media can be used for different purposes in the same geological cavern storage. Natural gas and carbon dioxide can be used as a storage medium and provide a basis for intertemporal arbitrage. Electricity itself is not storable in a cavern storage and has to be transformed into mechanical or chemical energy. Compressed air energy storages (CAES, adiabatic or diabatic) provide a mechanical solution to store electricity, by means of compressed air. An electrolyser is able to transform electric energy into easily storable chemical energy (hydrogen or methane). This is why the following analysis focusses on above mentioned storage media. The regional focus lies on Germany, since Germany, as single biggest market in the European Union, offers very liquid spot markets, subsequently the market data is very useful for an in-depth modelling of price developments. The findings of the following fundamental market analysis will be used to explain certain results from the econometric price modelling of electricity, natural gas, carbon dioxide and hydrogen markets

3.1 Electricity

The electricity market in Europe and especially in Germany has changed tremendously since the beginning of the liberalization of electricity markets in Europe in 1999. Due to stronger competition and the growth of a liquid electricity exchange (EEX), margins for electricity generators decreased and transparency grew, which is why, nowadays, the EEX prices are used as a benchmark for the entire electricity market including over-the-counter (OTC) trades (Rafal Weron, 2007, p. 15 f.).

A second big impact on the market structure has had the introduction of a subsidy policy for renewable energies (EEG) in Germany. This led and still leads to massive growth of renewable electricity production. In Germany, the gross electricity production from renewable energies had the biggest share of all electricity sources by surpassing lignite in 2014. Furthermore, the share of electricity generated by nuclear power is steadily decreasing since 2002 (Graichen, Kleiner, Litz, & Podewils, 2015). This is due to political decisions taken in 2002 and 2011 respectively, to phase out all nuclear power plants by 2022 (Gal, 2011).

Figure 1 maps the influence of price movements of different energy-related commodities on the average electricity price. The price paths of natural gas and coal are highly correlated. Both prices have peaks in the year 2008 with steep price drops following in 2009. The prices of natural gas lags about two months the price development of coal. This is mainly due to the fact that the gas market is less flexible and less interconnected worldwide, since the transportation of gas is far more difficult compared to coal and oil (mainly pipeline transport). After a sharp drop in 2009, a recovery of the coal price ended at the beginning of 2011 at around 100 €/t. Today's price is in the range of the deepest point in 2009. Gas prices increased steadily until the summer of 2012. From mid-2012 till the end of 2013 gas prices remained nearly constant. Since then, prices slid, excluding some seasonal effects, constantly.

The price development of Emission Allowances (EUAs) seems to be very much in line with the economic cycle. The price crashed during the financial crisis from 32 €/t_{CO2} in 2008 to 8 €/t_{CO2} in 2009. The pattern was highly correlated with the coal price movement. From the mid of 2009 until 2011 the carbon price stabilized at a level of 13-16 €/t_{CO2}. In the year 2011 the market participants expected that the slowdown of the GDP growth and decreasing energy growth due to the European debt crisis and the emerging share of renewable electricity production would lead to lower carbon dioxide emissions, thus lower demand for EUAs (see also). Prices dropped to levels below 4€/t in 2013. Since then, the prices steadily grew to about 8 €/t.

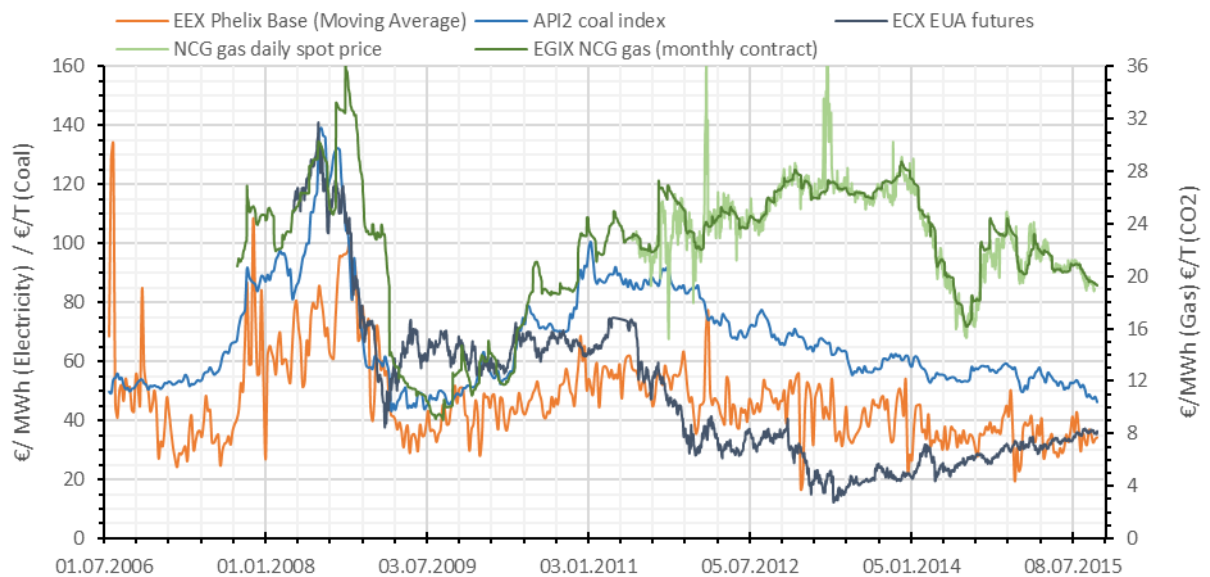


Figure 1: Price development of coal², electricity³, natural gas⁴ and European Emission Allowances over time. Source: own illustration, based on EEX (2015c), Reuters (2015a), Reuters (2015b), Reuters (2015c) and Quandl (2015).

All in all, a clear correlation between coal prices, prices of emission allowances and gas prices is visible. However, most importantly, in the long-run, electricity prices are also highly influenced by the behavior of energy and carbon prices. Even though the price path of electricity is very volatile from day to day due to fluctuating supply and demand, a peak in 2008 and a bottom price level in 2009 becomes clear. Along with the movement of energy commodities, electricity prices increased until 2011. Since 2011 a downward trend from 60 €/MWh towards levels below 30 €/MWh becomes visible. This trend is stressed by stochastic and seasonal movements.

The movement of energy prices over the last 9 years makes it hard to believe in a linear future trend of electricity prices. Many authors use the concept of constant drift / trend to model electricity prices. Linear trends are easy to model and estimate but yield unrealistic results for projections of prices over the timespan of 20 – 25 years. Subsequently, the following sections on price modelling of gas, emission allowances and electricity will not use constant trends but

² API2 coal index maps hard coal prices including freight and insurance costs to ARA harbours (Amsterdam, Rotterdam and Antwerp). The index is originally denoted in USD/t but is here converted to €/t with the historical daily €/\$-exchange rate.

³ In order to make the trend more visible a four-day moving average is applied to the daily baseload price of the Phelix-Index.

⁴ Due to a lack of market data of spot prices for natural gas (light green line) from 2006-2011, the EGIX natural gas index monthly contract is used to show the development over time. This index is based on rolling futures contracts in the NCG market area.

instead incorporate a cycling model of multiyear trends. This is believed to capture the real market movements superiorly, by modelling economic cycles.

To put it in a nutshell, long-term electricity price movements are mainly caused by economic growth cycles, which in turn leads to price movements in energy commodity markets and variation of electricity demand.

Renewable energies tend to be very volatile, which supports the magnitude and frequency of price jumps. Price jumps were, before the introduction of renewable energies mostly happening in an upward direction and never led to negative electricity prices. Nowadays, quite frequently, negative price jumps are occurring when an unexpected high influx of renewable energy meets a nearly static behavior of fossil-fueled power plants. Due to technical constraints, the sale of electricity with a negative price can be more economical than shutting down a fossil-fueled power plant (this is especially true for coal-fired plants) (De Graaf, 2013). Despite the occurrence of negative prices, electricity prices are highly mean-reverting, which means that electricity prices tend to move back quickly to the mean after a price jump.

Figure 2 shows the effect of seasonality on spot prices. On the one hand, average prices are higher in the winter due to higher energy demand. On the other hand, volatility is during the winter season also higher due to high infeed from wind energy with steep load gradients.

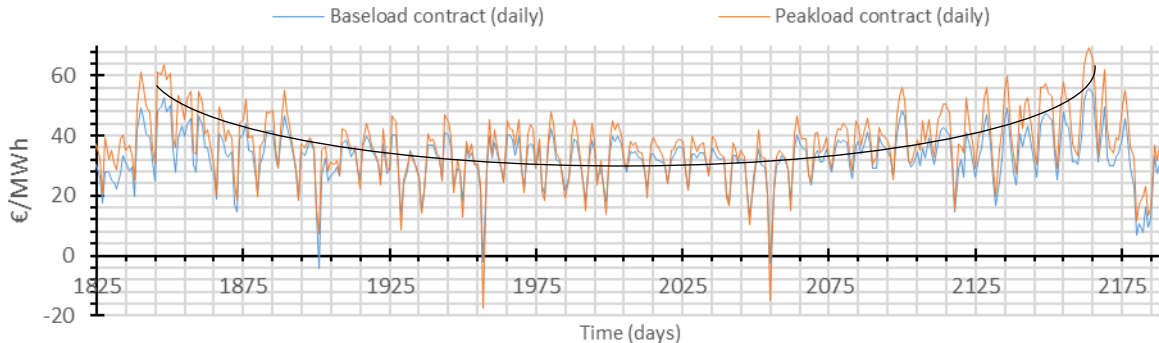


Figure 2: Spot price development on the day-ahead market (baseload & peak-load contract) at the EEX from 1.01.2009 - 2.09.2015, excerpt shown from 1.01.2014 – 1.01.2015. (EEX, 2015d, 2015e)

Moreover, figure 2 shows a weekly effect, too. Section 4 will give a more detailed view on the weekly and daily price movements. In a nutshell, the electricity market has the following properties (Muche, 2009): (1) High volatility; (2) Price jumps caused by price spikes; (3) Mean reversion; and (4) Seasonality.

The German electricity market is changing rapidly towards a more renewable electricity generation due to policy interventions. The German government aims to reach a share of renewable energies on the electricity generation of 55-60% by 2035. This share was 28% in 2014 (Bundesregierung, 2015).

Although the capacity of grid interconnections between boundaries of the European countries is increasing, the future energy system with high shares of renewables will not be able to work without storage facilities and residual fossil power plants. This is why the German policy maker are supporting the research and development of storage technologies (Bundesregierung, 2015).

Average baseload electricity costs are not expected to fall significantly below current levels (~30 €/MWh), since most fossil-fired power plants are currently hardly able to cover their marginal costs. Gas-fired power plants and older hard coal power plants are even put out of the market. Consequently, in the upcoming years several gigawatts of fossil electricity generation capacity is expected to be phased out (Dowideit, 2013). On top of this phasing-out of capacity that is out of the money, the remaining nuclear-based power plants are forced to be phased out gradually by law (Gal, 2011).

This is why, current price levels are expected to form the bottom line of future developments. A reduced amount of baseload plants and an increasing share of renewable energies increase the amount of extreme price spikes, as long as the remaining fossil-fueled power plants are not able to fully cover the load ramps of renewable energies and not enough electricity storages are installed to balance out sudden fluctuations.

In the section of price modelling the storage operator will trade at the EEX day-ahead hourly spot market PHELIX, which is the combined electricity market of Germany and Austria. One of main necessary assumption for the simulation is that the stochastic volatile behavior of electricity prices will remain similarly to the one seen in recent price movements at the hourly spot market. One has to keep in mind that this assumption is made based on a limited time period (approx. 6 years) with a focus on the German market. An increasing share of renewable energies in other European countries can either increase (more RE close to Germany) or decrease (geographically not close RE) the future volatility.

3.2 Natural gas

The natural gas market is, in contrast to other energy commodity markets, geographically quite regionalized. This is due to the fact that gas is not as easy storable as liquid or solid commodities. Natural gas can only be transported in liquefied natural gas (LNG) tankers or via pipelines. Since, large-scale LNG transport started emerging only a few years ago, the interconnection of prices on worldwide markets is rather limited (Rapoza, 2015).

Gas prices move in a seasonal pattern, since gas is traditionally used for the heating of houses, which leads to higher gas demand in winter than in summer (Carmona & Ludkovski, 2010). Moreover, the increased usage of gas-fired power plants as balancing units in times of

peak electricity demand gives an additional day-night pattern and intraday pattern in gas spot prices.

The monetization of the seasonality effect could be easily realized by a forward spread from July to January through a one-time transaction. Note, however, that an optimized trading scheme on the liquid and volatile spot market to use the day-night and intraday pattern, offers higher returns than solely seasonal trading along the forward curve (Carmona & Ludkovski, 2010).

The flexibility in the supply of gas can be met in three ways: (1) Adjusting the output of gas fields; (2) Line packing in extensive pipeline systems; and (3) Usage of large-scale gas storages.

The adjustment of gas field output is only possible if the gas fields are reasonably full and the distance to the grid connection not too far. Line packing, which increases the volume in the pipeline network by increasing the pressure, is frequently used. Though this type of “storage” is only applicable for small fluctuations, which could be balancing out the intraday demand pattern.

The stagnating demand for natural gas in Europe while production capacity and flexibility of Western European gas fields are decreasing, leads to a growing interest to invest in new gas storage facilities (Boogert & De Jong, 2008).

As figure 3 shows, the natural gas consumption is slightly declining in recent years. The total amount of gas consumed in the EU28 in 2013 was close to the natural gas consumption in 2000. The development of production and imports described in the last section becomes very clear:

In 2000 the EU-28 produced roughly as much gas as it imported. Nowadays, the EU28 imports roughly double the amount (12 EJ) as it produces locally (6 EJ). Most market participants expect this trend to continue, since many European gas fields are depleting and a shale gas boom as in the U.S. is not very likely.⁵

Consequently, the amount of natural gas produced locally will be at best at the level of recent years (if shale gas is used) or will further decline as in recent years (without shale gas). Due to the increasing share of heavily fluctuating renewable energies, an increased usage of flexible gas-fired power plants to balance out heavy load gradients is probable. In order to achieve the European emission reduction targets in the upcoming 25 years an increasing share of gas-fired plants in the remaining fossil-fueled generation facilities is necessary. Conse-

⁵ The public opinion on the technology to exploit shale gas, fracking, is in many European countries very negative, which is why it is not reasonable to assume that a boom of shale gas with such a massive impact on the gas market as in the U.S. is likely.

quently, an increasing volatility of gas prices at days with an increased usage of gas-fired plants is likely.

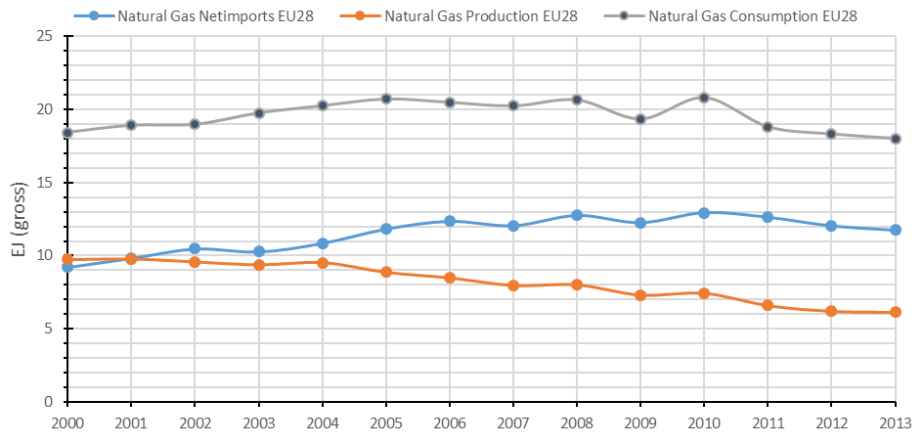


Figure 3: Sources and Consumption of Natural Gas in Europe (Eurostat, 2015)

On top of that, the increasing share of far-distance imports of natural gas leads to a higher vulnerability to delivery problems (Eurostat, 2015). A cold winter throughout Europe would cause not only a higher demand for natural gas in the western European countries but also in the eastern European and Eurasian-countries, which are often the transit countries of the most important pipelines to the west. As a consequence, the increasing need for natural gas in the transit countries will lower the amount of gas arriving at the end of the pipeline in Western Europe. This would lead to short-term price peaks, thus increasing the price volatility.

The intra-day and hourly gas markets in Germany (NCG and GPL) as well as in the Netherlands (TFF) have a low liquidity and no steady trading volume. This is why the price simulation will be based on day-ahead NCG gas spot market with a trading duration of 24h per trade.

3.3 Carbon dioxide

At first sight, carbon dioxide is not a typical commodity to use as storage medium to perform intertemporal arbitrage, but the European emission allowance market allows traders to perform exactly this arbitrage.

The European emission allowance market was established to reach emission reduction targets of the European Union. The main idea is that through only a limited amount of emission allowances the market price of allowances will find the cheapest solution to reduce emissions. The participant whose costs of saving carbon dioxide is lower than the market price of emission allowances (EUA) (in €t_{CO_2}) will generate a profit with the saving of emissions. There is an European cap on the maximum amount of yearly CO_2 emissions, which is currently lowered with a yearly rate of 1.74% to achieve the EU emission targets (Commission, 2015).

At the start of the EU emission trading system in 2005 nearly all EUA were allocated for free to the producing facilities based on their emission in recent years (grandfathering). In 2013, 20% of all yearly available certificates were auctioned, whereas the rest was allocated for free. Till 2020 the number of auctioned EUA is scheduled to increase to 60% and reach 100% by 2027 (EU, 2009).

Electricity generators already have to buy 100% of the needed EUA since 2013. The granted EUA are given to the emitting industries based on the emission of the best available technology in that specific industry. A cement-producing facility receives the exact amount of EUA which would be emitted by a modern and state of the art cement-producing facility (EU, 2009).

There are many exceptions to industry's obligations regarding specific emissions which are not accounted for (or certificates are given for free). Most exceptions try to avoid competitive disadvantage of exporting industries compared to worldwide producing facilities without emission trading systems.

The price development of EUA depends on several factors (Benz & Trück, 2009): (1) Annual decreasing amount of available EUA in order to reach politically set emission reduction targets; (2) Estimated and realized GDP development and development of fuel prices (influences CO₂ – output); (3) Market intervention of European Commission to adjust amount of EUA if prices turn out to be low; and (4) Number of EUA granted for free.

The overall emission of carbon dioxide in Europe is decreasing since 2006. The two largest European emitters, Germany and United Kingdom, follow the same decreasing pattern. A stronger dip of emissions in 2009 due to the financial crisis and an increase in 2010 due to the economic recovery disturbs this pattern slightly (Petroleum, 2015).

In consideration of the fact that a high price for EUA should trigger emission-saving measures, which in turn would reduce future emissions, the trend shown in figure 4 seems contradictory. The value of EUA has dropped sharply from 2008 to an all-time low in 2013. At the same time total emissions dropped nearly continuously. There are several theories why this market pattern is still logical and explicable, with the financial crisis in 2009 (causing an excess of EUA) and the increasing share of RE as main reasons. Statically, this explains only 10% of the price movement. The remaining 90% is still unclear (Koch, Fuss, Grosjean, & Edenhofer, 2014).

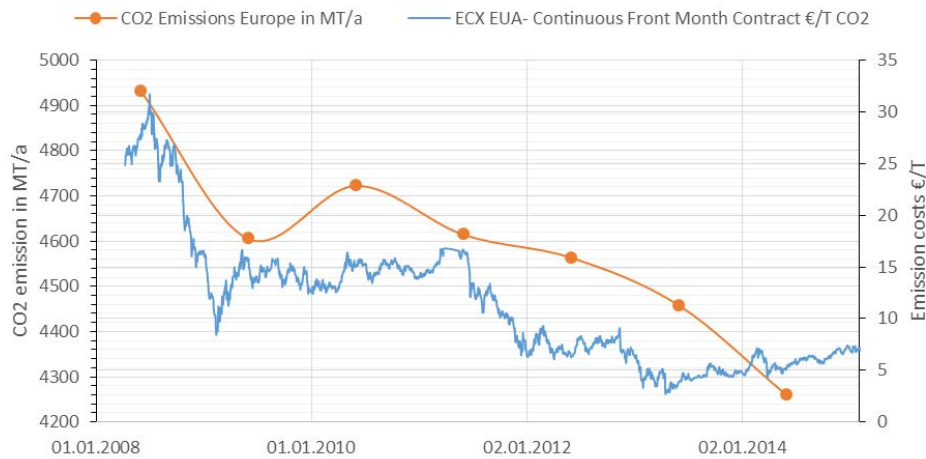


Figure 4: Price development of EUA from 2008 - 2015. CO2 emission in Europe in same time period for comparison. Source: Based on data from Petroleum (2015) and Quandl (2015)

The spot price path of EUAs experiences basically no extreme spikes and drops compared to natural gas spot prices or electricity spot prices. Moreover, the volatility from day to day is in absolute terms rather small (<1 €/t). Contrary to natural gas prices and electricity prices, recently, a clear upward trend is observable (figure 4). An excess of EUA led to a strong drop in prices during last trading phase II (2008-2012). At the beginning of trading phase III (2013-2020) in the spring of 2013, CO₂ prices reached its deepest point. Since then, the European Union has taken measures to reduce the excess EUA in the market to increase the average price level of EUA (Vassiliadis, 2015). The results are already visible in figure 4.

All in all, the future development of the EUA prices is highly dependent on political decisions and adjustments. Most importantly, the EU has two important targets on the reduction of greenhouse gases (Knopf, 2014): 40% emission reduction by 2030 (compared to 1990 emission levels); 80 – 95% emission reduction by 2050 (compared to 1990 emission levels).

This is why the maximum yearly amount of available EUA is reduced by 1.74% per year. From 2020 on, the yearly reduction rate will increase to 2.2% (BMUB, 2009; Commission, 2015). The potential impact of this policy is shown in figure 5. With the current reduction plan of the Emission Trading System (ETS), the emission targets 80% reduction compared to 1990 will not be achievable. Consequently, an even steeper decrease in yearly available EUA is foreseeable. This is in line with the plans of the European Union to increase the prices of EUAs by reducing temporarily the amount of available EUAs (Vassiliadis, 2015). Consequently, a long-lasting increase of EUA prices in the future is very likely.

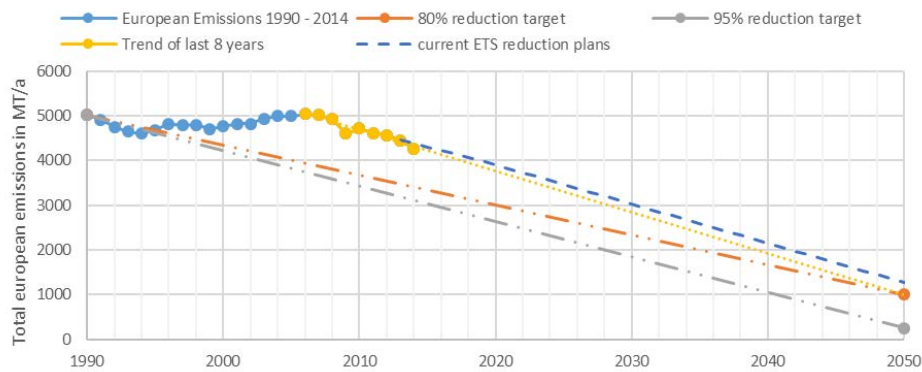


Figure 5: Emission pattern and European Emission targets. Source: Based on BMUB (2009), Commission (2015), Knopf (2014) and Petroleum (2015).

The following price simulation will be based on the market data from the secondary EUA spot market. EUA are traded every working day. Since EUA are without physical delivery, the emission allowances will be available after the settlement and can be used until the expiration date. The primary EUA market is designed as an auction with fixed auction dates. Auction prices are pretty in line with price levels at the secondary market, but auction dates are rare. Consequently, the historical prices of the secondary market will be used for simulation purpose.

3.4 Hydrogen

The hydrogen market is not comparable with the natural gas or electricity market. There is no hydrogen exchange, nor a large clearing house which established a hydrogen price index. Most of the produced hydrogen is used for industrial and chemical purposes, which is why the sale of hydrogen is basically a business to business transaction based on sealed-bid pricing (Saur & Ainscough, 2011). Consequently, a thorough market analysis as a basis for hydrogen price modelling is not possible. From an economic perspective is the usage of hydrogen as storage medium not reasonable until a liquid hydrogen market evolves. Apart from the very limited market size and liquidity for hydrogen, there are also several technical properties which reduces the suitability of hydrogen as storage medium significantly. These properties are explained in section 5.2.4 below.

4. Storage media: modelling and simulation

The following subsections give an overview of different modelling approaches and describe and the most suitable approaches for electricity prices, natural gas prices and carbon dioxide prices. To perform intertemporal arbitrage with a cavern storage the most efficient, a storage operator with a suitable storage has to be able to switch between injection and withdrawal within an hour (Barbour et al., 2012). This technical constraint allows to trade on a spot mar-

ket, which has a much higher volatility than forward markets. The value of a storage increases with higher volatility (Boogert & De Jong, 2008). As basis for the following price simulations, the capability of hourly switching will be assumed. A Monte Carlo approach is incorporated in every price simulation in order to account for the stochastic nature of the price processes.

4.1 Electricity

The following subsections will describe the mathematical approach to decompose the historical price data in order to simulate future electricity price paths. Section 2.2 gave an extensive overview of different price simulation approaches. In this study a hybrid model consisting of Markov regime switching approach (*reduced form model*) and a similar day method (*statistical model*) are used. The algorithm to model a Markov three regime switching approach, which will be used in this study, can be found in Janczura and Weron (2015). The overall approach is pretty much in line with the findings of Janczura et al. (2013). A modified similar day method will be used to identify and remove the weekly pattern, while a sine function identifies and removes the long term pattern.

The fundamental type of models, just as most other models described in section 2.2, will not be used in this study. However, some fundamental data discussed in section 3 will be used to test and explain findings based on stochastic models applied below.

Keles, Genoese, et al. (2012) and Rafał Weron (2014) give an extensive overview of approaches to model stochastically realistic spot prices. Most price models are based on logarithmic prices to simplify calculation and better incorporate price spikes. Consequently, these price models cannot incorporate negative prices (Keles, Hartel, et al., 2012). Negative prices occur quite frequently at the German spot market (PHELIX), which is why certain price models have to be changed in order to appropriately describe the true price movement. In order to model the stochastic component appropriately, the Markov regime-switching model requires deseasonalised spot prices. There are many different approaches to extract the long-term seasonal component from the dataset (Nowotarski, Tomczyk, & Weron, 2013). Z. Chen and Forsyth (2010) extend the model of Boogert and De Jong (2008) by including an additional seasonal component to the mean reversion model:

$$dP = \kappa(\mu_0 - P)dt + \sigma P dW(t) + S(t)P dt \quad (6)$$

with μ_0 as long-term equilibrium price and $S(t)$ as a sinusoidal shaped seasonality component. Huisman et al. (2007) extend the seasonal component with a hourly and weekly component, but use the same mean-reverting process as Z. Chen and Forsyth (2010). Holland (2008) models $\mu(t)$ with a sinusoidal shape to incorporate annual and semi-annual fluctuations:

$$\mu(t)dt = \alpha(A + \beta_A * \cos\left(2\pi\left(\frac{t}{365} - \frac{t_A}{365}\right)\right) + \beta_{SA} * \cos\left(4\pi\left(\frac{t - t_{SA}}{365}\right) - S_t\right) \quad (7)$$

Pilipovic (2007) proposes a sinusoidal approach to model the seasonal pattern of the electricity price. Rafal Weron (2007) advocates a similar approach and tries to model the seasonal effect with a multiple sine function to incorporate all possible discrete frequencies. The function is as follows:

$$x_t = a_0 + \sum_{k=1}^n [a_k \cos(\omega_k t) + b_k \sin(\omega_k t)] \quad (8)$$

The above-mentioned approach of multiple sine functions will be used in the subsequent section to estimate the long-term and seasonal cycle.

Weron (2007) applies in his book several techniques to decompose the weekly and daily cycle: (1) Mean or Median week (Janczura et al., 2013); (2) Moving Average Technique; (3) Rolling Volatility Technique; (4) Wavelet Decomposition.

The *Moving Average Technique* yields very good results but has the problem that it is difficult to use the results from the decomposition of historical data to simulate future prices (Janczura et al., 2013). The *Rolling Volatility Technique* is mainly useful to approximate a pattern if only few data points are available. Wavelet Decomposition serves as an alternative to the Fourier Transformation. It is composed as a series of Daubechies functions. It is able to model historical data very precisely, but is not suitable for long-term projections (Janczura et al., 2013). In this study, the Wavelet Decomposition is used to deseasonalize the data in the first place by means of an algorithm which can be found in Janczura and Weron (2015). For the reconstruction of the deterministic part of the price path the concept of a Median Week is used. An algorithm developed by Rafal Weron (2007) incorporates this concept. The main idea is to find an average daily pattern for each day of the week. This weekly pattern can be replicated infinitely many times, consequently, a weekly and daily pattern even for long-term price projections is no problem. The overall price will consist of two main components, a deterministic part and a stochastic part. The deterministic part describes all patterns which follow a continuous, repeating movement, while the stochastic part tries to map all random price movements:

$$P_t = P_{det} + P_{stoch} = (P_{ltc} + P_{ssc} + P_{stc}) + P_{stoch} \quad (9)$$

The following price patterns are identified:

Multi-year, long-term pattern (ltc)

As explained in section 3, the development of the long-term electricity price is subject to the economic growth and the development on the energy commodity markets. Consequently, a long-term pattern, as shown in figure 6, can easily be identified.

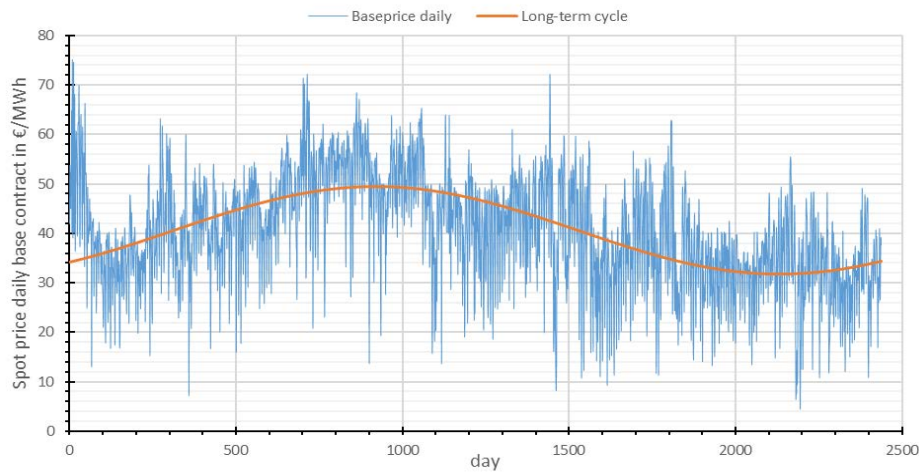


Figure 6: Development of the average daily electricity spot price from 1.01.2009 - 2.09.2015 - outliers removed⁶. Fitted with sinusoidal long-term cycle. Based on data from EEX (2015d)

Figure 6 also shows the result of the Fourier fit graphically and table 2 shows the exact regression results.

Table 2: Regression results to estimate the long-term cycle. Based on average daily spot price data

Variable	Coeff.	[95% confidence interval]				
a_0	40.6	40.16	41.04	R^2	0.4328	
a_1	-6.451	-7.279	-5.623	Adj. R^2	0.4321	
b_1	6.101	5.24	6.962	RMSE	9.1	
W	0.002592	0.002488	0.002696	SSE	$2.014 \cdot 10^5$	

The long-term cycle has a periodicity of approx. 2424 days. This is about 6.64 years and is in line with the length of an economic cycle, which is assumed to take between 5 and 8 years.

Seasonal pattern (ssc)

Electricity demand is also fluctuating seasonally. Traditionally, there is higher demand during the winter due to e.g. more need for lightening, but recently the effect has become less significant. This is due to the fact that the highest average wind speed is achieved during the winter. Consequently, the massive increase in available wind turbine output dampens the increase of electricity prices during the winter (see figure 7).

⁶ To improve the graphical appearance outliers outside of the interval of $[\mu \pm 3\sigma]$ were removed of the base price dataset. The regression results are based on the original dataset.

Table 3: Regression results to estimate the seasonal cycle. Based on data of average daily spot price

Variable	Coeff.	[95% confidence interval]			
a_0	0	-0.073	0.073	R^2	0.4303
a_1	3.123	3.017	3.228	Adj. R^2	0.4303
b_1	0.3717	0.1673	0.5761	RMSE	8.928
w	0.0007	0.0007	0.0007	SSE	$4.659 \cdot 10^6$

Figure 7 and table 3 show the outcome of the Fourier fit. The seasonal cycle has a periodicity of approx. 8540 hours (= 0.97 years) and an amplitude of approx. 7 €/MWh.

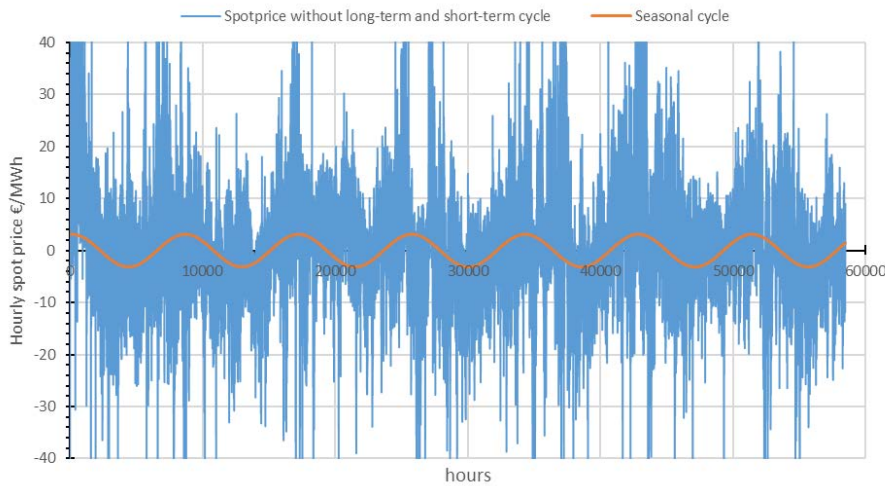


Figure 7: Development of hourly electricity spot price from 1 Jan 2009 – 2 Sep 2015. Without long-term and short-term cycle. Fitted with sinusoidal seasonal cycle. Source: Own illustration, based on EEX (2015a)

Daily pattern (stc)

Due to varying demand during the day, prices follow a certain pattern throughout the day with lows during the night and peaks mainly during the morning and evening hours (see figure 8).

Weekly pattern (stc)

Throughout the week, hourly spot prices follow the path of a work week. During the weekend less people are at work and less production facilities are running, which leads to lower electricity demand (see figure 8). On Mondays the price rises gradually until the regular start of a working day (8-9 am). The electricity price simulation process can be found in the appendix A1. The residual stochastic price path in figure 33 (A1) is the result of the removal of daily, weekly, seasonal and long-term cycles. In terms of regimes, one is able to identify sudden drops, spikes and a very frequent stochastic behavior in the base regime.

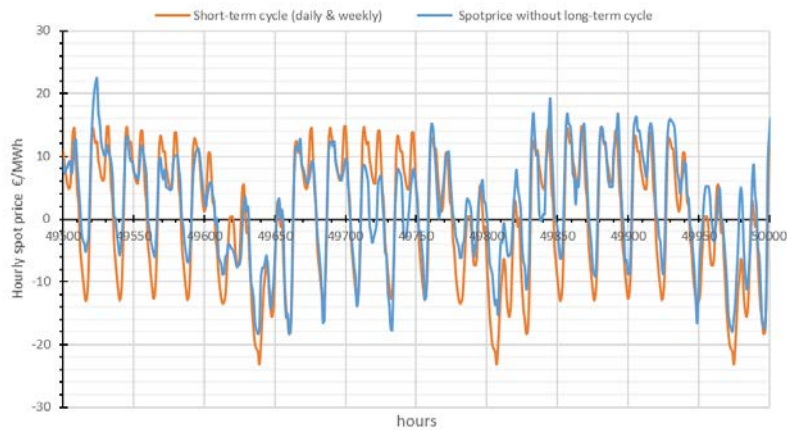


Figure 8: Development of hourly electricity spot price in detail, fitted with short-term cycle based on algorithm developed by (Janczura & Weron, 2012).

Figure 9 shows one simulated price path compared to the real historical price path. The simulated price path seems to fluctuate a bit more frequently, but has similar extreme price movements. The aim of a stochastic model, which chooses the stochastic behaviour with random generated numbers, is not to gain exactly the same price at time t but rather to reproduce a similar pattern over time. The results presented below are satisfying and will be used as the basis to estimate the value of a storage cavern over time.

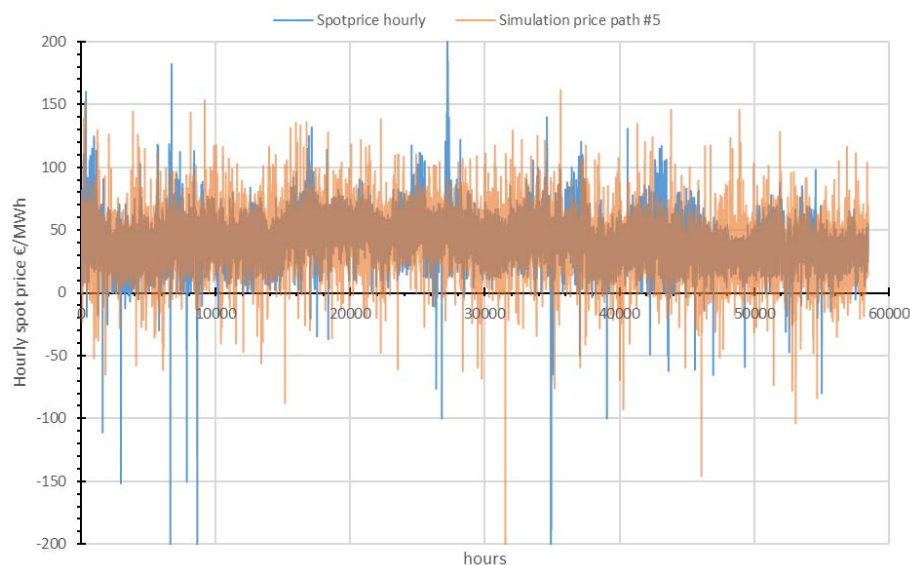


Figure 9: Comparison of historical hourly data (EEX, 2015a) with the simulation results of price path no. 5 (out of 500 runs).

4.2 Natural gas

The theory on price modeling of natural gas is, from a technical perspective, not different from the modelling of electricity prices described in section 4.1. This is why Carmona and Ludkovski (2010) and Eydeland and Wolyniec (2003, p. 136 ff) propose several possible price models suitable to trace the price movements on natural gas markets, such as the simple

Markovian stochastic differential equation with a Brownian motion, mean-reversion models and jump-diffusion models.

There are some smaller differences which overall cause a slightly simpler modelling approach: (1) No negative prices; (2) No liquid hourly spot market; and (3) Less intense spikes and nearly no drops. The seasonality of natural gas prices and the existence of a long-term cycle allow the use of a similar approach as in section 4.1. Although the available data allows only an assessment of daily prices, the mean week strategy can still be used, since gas prices follow a similar weekly pattern as electricity prices. The fact that gas prices experience nearly no extreme drops makes the usage of a Markov Regime Switching approach with three regimes obsolete. Two regimes are enough to account for frequent extreme price spikes.

Although the GPL (Gaspool) market area includes the most suitable geological site for salt cavern storages in Germany (see figure 10), the historical spot price path for the simulation is taken from the daily reference price of the NCG (NetConnect) market area. The GPL spot market is less liquid than the NCG area. Since the prices on both markets only differ marginally, no major adverse impact on the validity of the outcome has to be expected.



Figure 10: Market area of gas grid operators in Germany (Gas, 2015)

Multi-year, long-term pattern (ltc)

As explained in sections 3.1 and 3.2, the development of the long-term natural gas price is subject to the economic growth and the development on the energy commodity markets. These markets follow cyclic demand and supply patterns.

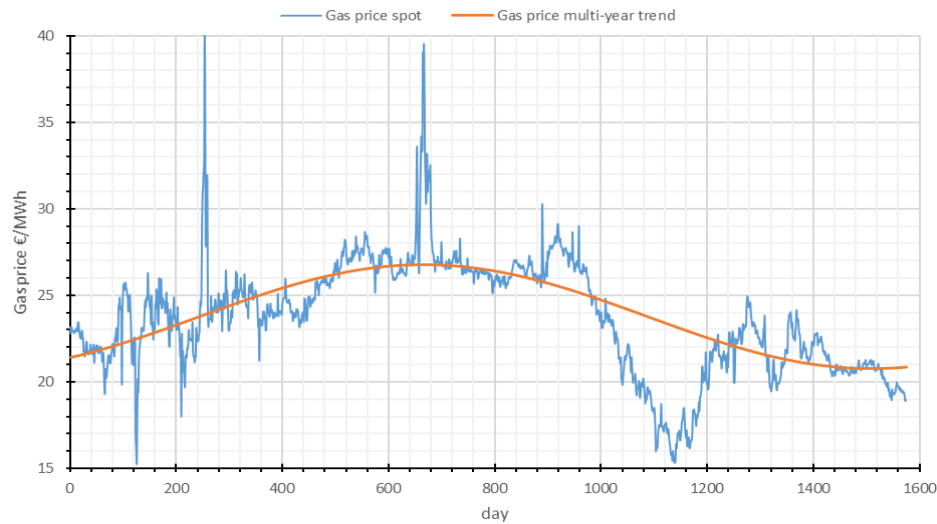


Figure 11: Development of natural gas prices at NCG-Hub and ltc from 31 May 2011 – 21 Sep 2015 (EEX, 2015c)

As Figure 11 shows, a multi-year trend on the gas spot market is clearly visible through a Fourier fit. The long-term cycle has a periodicity of approx. 1683 days. Consequently, each cycle takes about 4.61 years, which is smaller than the expected economic cycle. The results and coefficients of this regression (P_{G-ltc}) are shown in figure 11 and table 4.

Table 4: Regression results to estimate long-term cycle.

Variable	Coeff.	[95% confidence interval]			
a_0	23.79	23.65	23.92	R^2	0.7953
a_1	-2.364	-2.536	-2.192	Adj. R^2	0.7949
b_1	1.831	1.551	2.112	RMSE	1.467
w	0.0037	0.0036	0.0039	SSE	3382

Seasonal pattern (ssc)

Gas demand is also fluctuating seasonally. Traditionally, there is higher demand during the winter due to the fact that a big share of the gas consumption is used for heating. Since the supply of natural gas is rather constant throughout the year and limited by the maximum flowrate of the long-distance pipeline network, the demand surpasses the supply during winter. The shortage in supply is compensated by the withdrawal of natural gas from storages. These storages are charged during the summer and discharged during the winter.

Figure 12 shows that the seasonal cycle of the natural gas price is not as significant as for electricity. This is due to the fact that the seasonality depends on the temperature development during the winter. If the winter turns out warmer than expected, a price drop during the spring and summer follows, because the storages are still nearly full (Stronzik, Neumann, & Rammerstorfer, 2008). Consequently, excess gas in the market has to be sold with a discount.

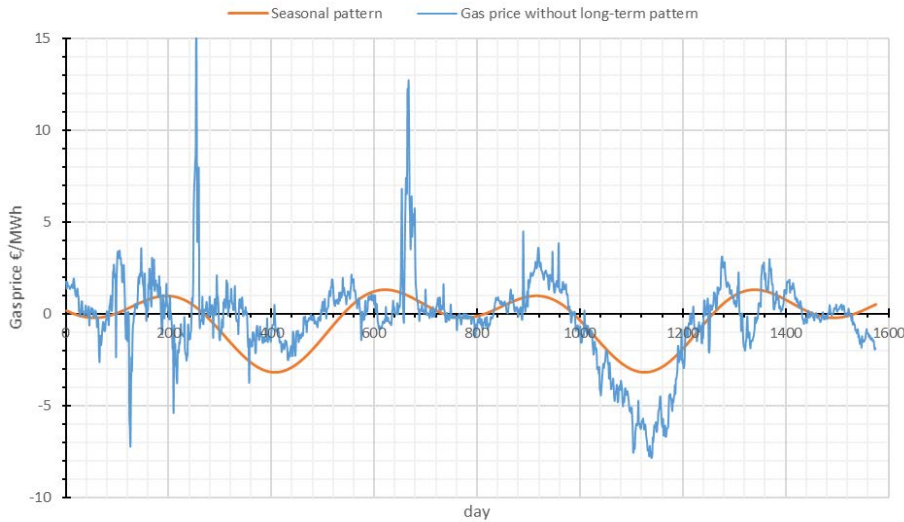


Figure 12: Price path of natural gas after the removal of the long-term cycle. Seasonal cycle fitted (EEX, 2015c)

The regression was conducted with a Fourier fit consisting of two sine-cosine combinations. The overall periodicity is approx. 760 days but the time from peak (winter) to peak (winter) depends on the length of the cold season (either approx. 295 days or 424 days). Results and coefficients of this regression can be seen in figure 12 and table 5, respectively.

Table 5: Regression results to estimate seasonal pattern

Variable	Coeff.	[95% confidence interval]			
a_0	-0.2706	-0.3387	-0.2025	R^2	0.6384
a_1	1.099	0.9995	1.199	Adj. R^2	0.6372
b_1	-0.1436	-0.264	-0.0233	RMSE	1.374
a_2	-1.122	-1.223	-1.021	SSE	2961
b_2	0.2909	0.1018	0.4801		
w	0.008269	0.008176	0.008362		

Weekly pattern (stc)

Throughout the week, daily gas prices follow the path of a work week. During the weekend less people are at work, less production facilities and gas-fired power plants are running, which leads to lower gas demand (see figure 13). In contrast to electricity, the short-term pattern suggests that the mean prices on Mondays are the highest of the entire week. It has to be said that the short-term pattern is not as significant as in the electricity market. Not only the fit is worse but also the overall price difference is, with an amplitude of approx. €0.4, rather small. The exact sequence of the price simulation is shown in the appendix.

The residual stochastic price path in figure 34 (appendix) shows the result of the removal of all recurring patterns. In terms of regimes, one is able to identify sudden spikes and a very frequent stochastic behavior in the base regime. The overall remaining amplitude is rather small (approx. €1-5).

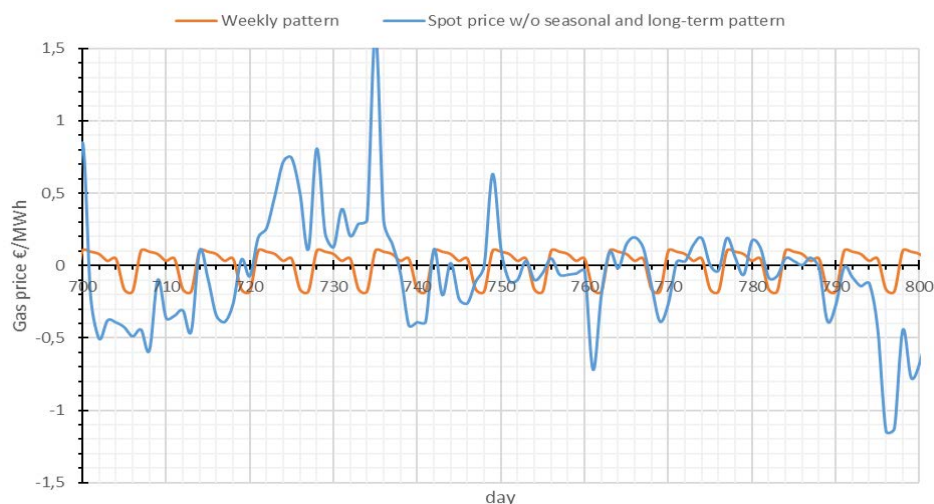


Figure 13: Residual gas price path without seasonal and long-term pattern. Weekly cycle fitted on data. Data from 31.05.2011 – 21.09.2015. This extract is from 30 Apr 2013 – 08 Aug 2013 (EEX, 2015c)

Figure 14 shows one simulated price path compared to the real historical price path. The simulated price path is very much in line with the real world price movement. Sudden price spikes are visible and the volatility seems very similar. The aim of a stochastic model, which chooses the stochastic behavior with random generated numbers, is not to gain exactly the same price at time t but rather to reproduce a similar pattern over time.

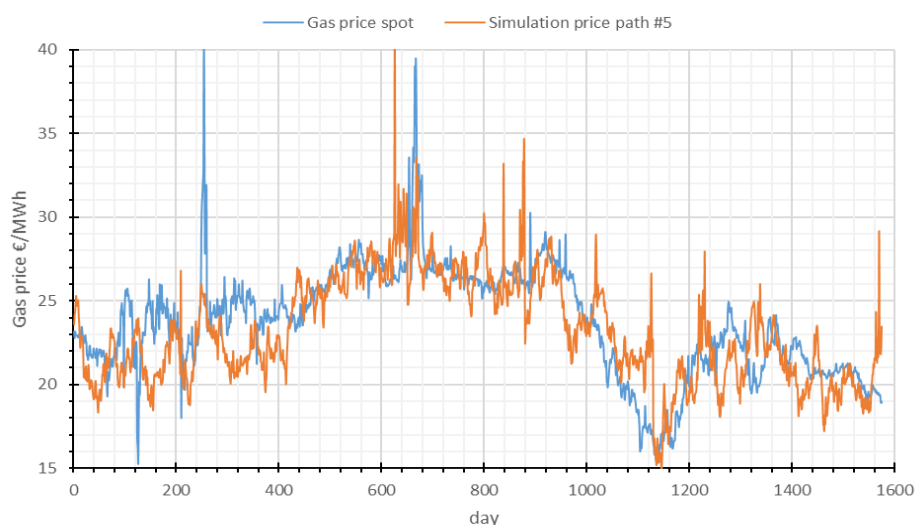


Figure 14: Comparison of historical gas price data with the simulation results of price path no. 5 (out of 500 runs).

The results presented above are very satisfying and will be used as basis to estimate the value of a storage cavern over time.

4.3 Carbon dioxide

Benz and Trück (2009) analyzed EUA market data from the OTC trades in the year 2005 and 2006 to test two price processes: a Markovian regime switching (MRS) approach and a autoregressive-GARCH approach. The regime switching approach with two regimes turned out to

fit better on the market data. Further findings were that no clear seasonal or weekly cycles were visible (Benz & Trück, 2009). This is a logical finding, since EUA have an expiry date of several years and there is no need for real-time balancing, consequently no time-critical usage of EUAs is expected.

In principal all modelling concepts presented in the sections of electricity price modelling (4.1) and gas price modelling (4.2) are applicable. Since there are no extreme price spikes or drops (Figure 15) there is no need for a MRS-(3-regime)-approach and a Markov base regime (Brownian Motion) with drift correction is sufficient (see also Boogert and De Jong (2008)).

As described in section 3.3, due to a constant decreasing number of yearly available EUA, a long-lasting increase of EUA prices in the future is very likely. This is why the following paragraphs will not only develop a price model based on historical patterns but will also describe two alternative scenarios with stronger price increase. Based on the estimations of NEP (2013) and Prognos (2013), the following regression results are adjusted to achieve a larger inclination of the price path.

Historical spot price data from the secondary market for carbon emission allowances (ECX EUA secondary market) has been used to model the price development. Missing data during the weekends and public holidays was filled with prices from the moving average of surrounding days. Although the secondary market is still pretty illiquid at certain points of time, the price movement of the secondary market is very close to the movement of the primary market. Since the primary market has far less trading days, the usage of the secondary market data seems a better approach.

Multi-year, long-term trend

The data on the spot prices of EUAs traded at the secondary market shows a significant long-term trend. This trend can be approximated with an inverse power function (root function), which represents a limited growth process. With the parameters found, the fit the function grows steadily and achieves a level of approx. 12 €/t after 3500 days and level of 15 €/t after 6500 days. A second, exponential, function describes the drop in the first 100 days accordingly. The result is shown in figure 15. The combined trend is constructed out of the following combined function:

$$P_{CO2-trend} = a * x^b + c * e^{d*x} \quad (10)$$

The exact sequence of the price simulation is shown in the appendix. Results are shown in Table 6, table 7 and figure 15.

Table 6: Regression results of power fit

Variable	Coeff.	[95% confidence interval]					
a	0.6177	0.5768	0.6587	R ²	0.8179	RMSE	0.5633
b	0.3641	0.3537	0.3745	Adj. R ²	0.8177	SSE	314.8

Table 7: Regression results of exponential fit

Variable	Coeff.	[95% confidence interval]					
c	5.441	5.136	5.746	R ²	0.7026	RMSE	0.4999
d	-0.02306	-0.02486	-0.02125	Adj. R ²	0.7023	SSE	247.9

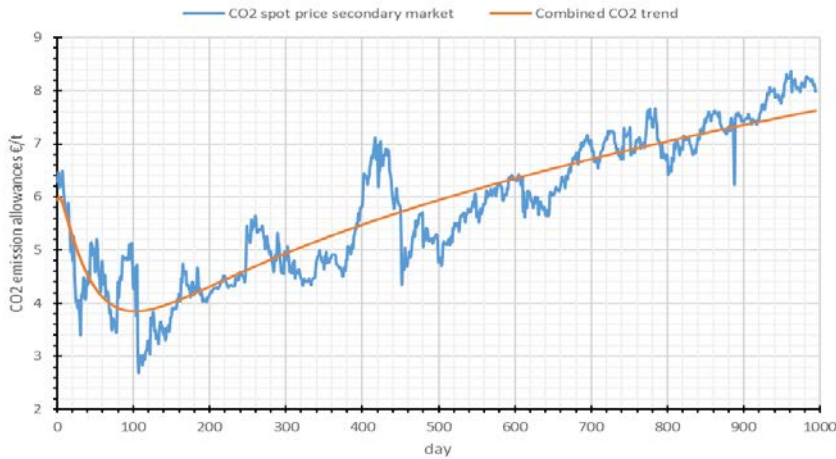


Figure 15: EUA spot price in secondary market and trend fit. (EEX, 2015b)

After removing the long-term trend, the residual stochastic path as shown in figure 35 (appendix) is left. The stochastic path is less spiky than the residual paths of electricity (figure 33) and gas (figure 34). Only one value over the timeline can be identified as spike [$P \geq \mu + 3\sigma$] (Janczura et al., 2013). Consequently, only one stochastic process is needed to map the historical price path.

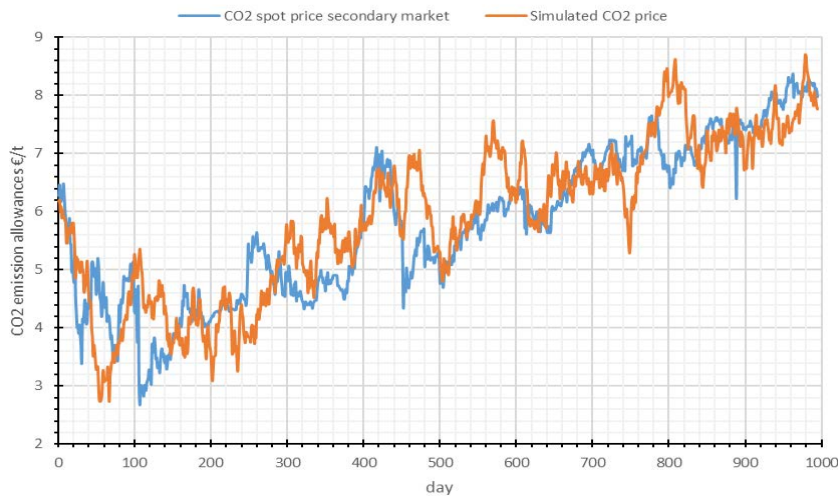


Figure 16: Comparison of historical EUA price data (EEX, 2015b) with the simulation results of price path no. 5 (out of 500).

Figure 16 shows one simulated price path compared to the real historical price path. The simulated price path is very in line with the real price movement. The trend is clearly visible and the volatility seems very similar. The aim of a stochastic model, which chooses the stochastic behavior with random generated numbers is not to gain the exact same price at time t but reproduce a similar pattern over time. The results presented below are very satisfying and are in line with the expected steady increase in prices for EUAs. This data will be used as basis to estimate the value of a storage cavern over time.

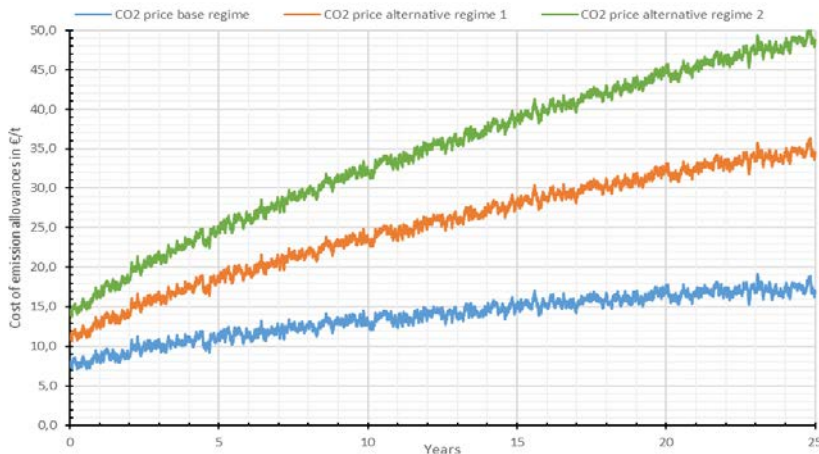


Figure 17: Price path of simulated CO₂ prices and alternative price paths based on estimations of Prognos (2013), NEP (2013) and Fraunhofer (2013)

Figure 17 describes not only a price path as a result of the CO₂ price simulation described above, but shows also two alternative price paths based on the estimated upper and lower bound of CO₂ prices used in the study of Fraunhofer (2013). The additional price paths are estimated through the manipulation of the regression parameters of equation (10).

The alternative regimes 1 and 2 will also be used in the following storage valuation to determine the impact of higher CO₂ prices on the value of the storage applications.

5. Geological cavern storage

Geological storage can be classified into pore storages and cavern storages. Saline aquifers and depleted oil and gas fields are pore storages whereas cavern storages are artificially made caverns in solid soil.

Natural gas is stored in naturally available small cavities (pores). The deeper the pore storages the higher the storable volume since the storage pressure increases with depth. The optimal depth is a trade-off between technical properties and restrictions and associated costs, which is why the most favorable depth is often seen in the range of 500 – 1000m (Stronzik et al., 2008).

Cavern storages are artificially made hollow spaces. They can be mined in rock layers (mined cavern) or solution mined in salt layers (salt cavern). Most commonly used are salt caverns since the solution mining process is rather cheap and a mature technology. The size of each cavern is limited due to mechanical constraints. To increase the overall storage volume, there is often a field of salt caverns (>10) mined in the same salt deposit (Stronzik et al., 2008). Caverns are not only made for storage purpose but also to extract salt and as waste deposits (Struck, 1993).

Large-scale storages can be described by its operational constraints: working volume, base gas requirement, injection and withdrawal rates and associated variable and fixed costs. Dependent on the type of storage some operational constraints are more favourable than others (Thompson et al., 2009).

Depleted oil and gas fields are often large and cheap to transform into a storage since most of the needed infrastructure is already available. Moreover, the fields contained gas or oil for millions of years, consequently the risk of leakage is very low. However, the flexibility is mostly poor due to limited injection and withdrawal rates and the need for cushion gas is often rather high (ratio of working gas to total volume is low) (see also table 8).

Saline aquifers are smaller than depleted reservoirs but have a high risk of leakage since these facilities are more difficult to map. The working gas ratio is rather low (20-35%) compared to cavern storages and depleted reservoirs. Saline Aquifers are the least flexible storages in this comparison (table 8) but the geographically most spread (Boogert & De Jong, 2008; Maragos & Ronn, 2002).

Salt cavern storages are rather easy exploitable but need deep geological salt layers which limits the usage to certain geographical areas. Most favourable locations are in north-west Germany (Struck, 1993). The technical properties of salt itself prevents leakages and enables a high flexibility by high injection and withdrawal rates (Sørensen, 2007). The theoretical leakage rate of salt caverns is in the range of 0.01% p.a. (Crotagino et al., 2010).

Table 8: Comparison of different storage types (Crotagino et al., 2010; Gillhaus, 2010; Sørensen, 2007; Stronzik et al., 2008; Struck, 1993)

	Saline aquifer	Depleted reservoirs	Salt caverns
Working gas volume in Germany (V_n in 10^6 m ³)	30 - 1085	100 - 4,600	50 – 120 /cavern
Share of Cushion Gas [%]	65-80	50	20-30
Cycle times	1	1-2	5-12
Construction time [a]	4	2	2-10
Injection/withdrawal rates	Low	Low	High
Daily Deliverability	0.5%	1%	Up to 10%

As table 8 proves, salt caverns are the most flexible large-scale geological storages. Since the main focus of this study is to find the most valuable medium to perform intertemporal arbitrage, the following sections will focus on salt caverns as most suitable storage.

If a cavern is used for daily charging and discharging as in this paper assumed, it is important to consider that due to higher thermal and pressure stresses not every existing gas cavern is able to be used for high frequency charging and discharging (Zander-Schiebenhöfer et al., 2015). The following sections about costs and technical restrictions will only include salt cavern storages which can be regarded as high deliverability multiple cycle (HDMC) facilities. These facilities can switch from injection to production within minutes and have steeper ramp rates (change of flowrate) than any other power generation unit (Barbour et al., 2012; Gill & Cowan, 2014).

Traditionally, most salt cavern storages were owned by utilities as gas storage to balance seasonal fluctuating demands. Due to the deregulation of the electricity and gas markets in Europe the natural gas storage services are nowadays unbundled from the sales and transportation services. Since storage is charged as a separate service and the recent development of liquid spot and future markets for gas and electricity, intensive research on value maximizing operation modes started about 15 years ago (Boogert & De Jong, 2008). The International Energy Agency estimated in 2004 that the global underground gas storage capacity will double in the next 30 years (2000–2030) due to falling indigenous production and steady (Europe) or increasing gas demand (US, Asia) (Boogert & De Jong, 2008).

But cavern storages can also be used as electricity storage through the usage as a compressed air energy storage (CAES) or to store either hydrogen or carbon dioxide. The technical properties will be discussed in section 5.2 and the associated costs in section 5.3.

5.1 Potential storage sites

The technical process of solution mining to construct caverns in salt layers was first used in the USA and Canada after the Second World War. The first gas cavern storage in Germany was established at the beginning of the 1970s in Kiel (Struck, 1993).

Most gas cavern storages can be found in north-western Europe since these regions possess geotechnical favorable thick bedded and dome-shaped salt formations. The majority of caverns are used for gas storage while some are used as strategic oil reserves. Only one site is used as a CAES in Huntorf, Germany (Struck, 1993), which was world's first CAES in 1978. As figure 18 shows, many European countries use salt cavern fields for storage purpose, but the majority of all storages, especially gas storages, are located in Germany due to its favorable salt deposits. The area of the most favorable Zechstein salt deposits in suitable depths as

dome formation can be found in north-eastern Netherlands, north-western Denmark and Central Poland (Gillhaus, 2007).

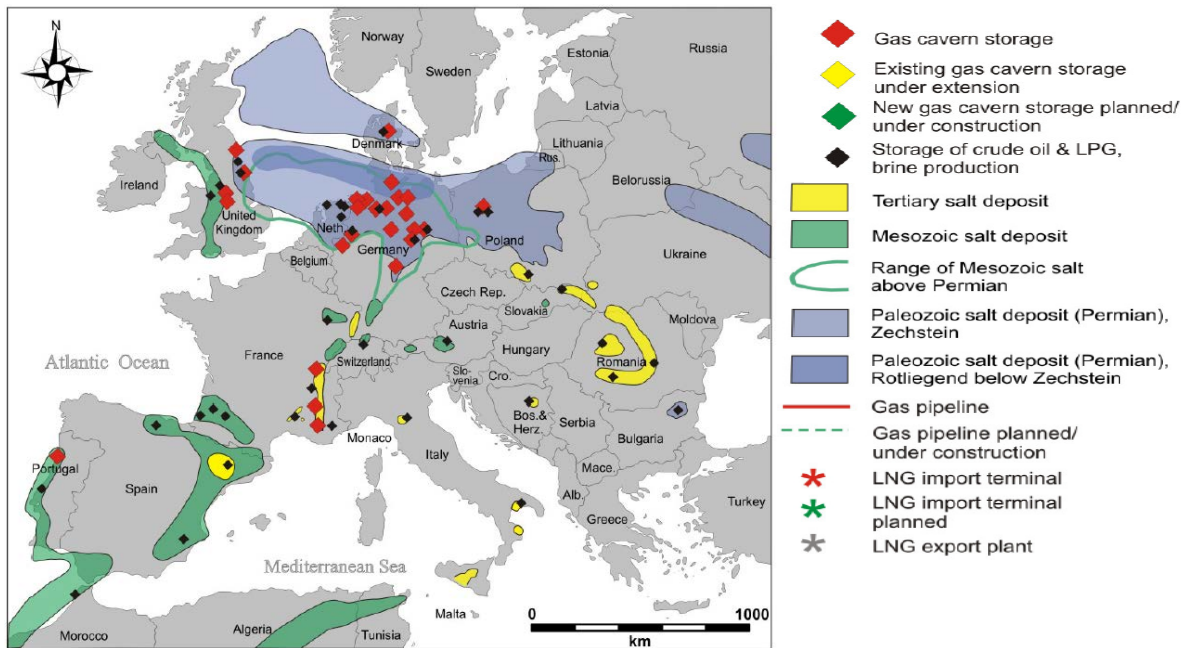


Figure 18: Salt deposits and cavern field in Europe (Gillhaus, 2007)

Since Germany is a major country for gas transit and at the same time the biggest consumer of natural gas in Europe, major gas pipelines run through Germany. Consequently, the vast amount of storage facilities in northern Germany has a strategic explanation.

Salt domes are most preferable because of the homogenous vertical expansion. Caverns in salt domes can reach the optimal shape with a height to width ratio of about 10:1. The height can reach up to 600 m and the width 60-100 m. Most caverns have volumes in the range of 500,000 – 800,000 m³, which can lead to working gas volumes (depending on pressure) for natural gas of 100 – 120 million m³ (V_N) (Gill & Cowan, 2014; Gillhaus, 2007; Hannover, 2014).

As figure 18 shows, Europe has in terms of suitable salt deposits still enough potential for further increase in salt cavern storages. The competition will be on the exploration of the salt deposits with the most favorable salt layers and the infrastructure already in place (high voltage grid, gas pipeline) (Raju & Kumar Khaitan, 2012).

In order to promote and map the potentials in detail, the German government is funding a research project which analyses all potential suitable sites in Germany and map them in a geographic information system (GIS). The focus lies especially on potential CAES sites, which need HDMC-ready salt layers (BMW, 2015).

5.2 Technical properties and restrictions of salt cavern storages

The technical challenge during the construction of a salt cavern is to mine a self-sustaining cavern which is as big as possible and able to withstand high pressure and high pressure gradients without any help of supporting construction elements. To avoid leakage due to salt fracturing, the maximum pressure level may not be exceeded (Struck, 1993). The maximum pressure limits the maximum storable amount. The maximum pressure in salt caverns is defined as approx. 80% of the initial formation pressure at the depth of the cavern roof⁷. For most existing caverns the maximum pressure is in the range of 15-20 MPa (Sørensen, 2007; Struck, 1993)

The minimum approved pressure is limited to retain the shape and structure of the cavern with the help of cushion gas. To avoid structural damage, the minimal pressure is approx. 30% of the maximum pressure (Crotogino et al., 2010). Not only are the minimum and maximum pressure limited but also the cycling frequency. Creep behavior of salt particles limits the pressure gradients, which in turn define the possible cycling frequency. If the capability of creep is high, less pressure gradients are allowed and vice versa (Struck, 1993).

For cavern construction large amount of freshwater is needed and a brine disposal system has to be in place. This is why most existing cavern sites are preferable located close to a shore or a river where the diluted brine can be easily disposed.

The amount of storable energy in a mined cavern depends on the one hand on the cavern size. The assumed cavern has a working gas volume of 77,500,000 million m³ (V_N -standard volume)⁸. This corresponds to a void volume of approx. 500,000 m³. On the other hand, the storable energy depends on the caloric value [MJ/m³] of the stored gas, too.

The biggest advantage of caverns over other storage types is the high injection and withdrawal rate. The state of the art salt caverns in Germany have withdrawal rates of 150,000 – 200,000 m³/h (V_N) and injection rates of 75,000-100,000 m³/h (V_N) (Hannover, 2014). Storages in use for CAES have even higher discharge rates in the range of 700,000 m³/h⁹

5.2.1 Compressed Air Energy Storage (CAES)

Compressed air storages store mechanical energy by means of the transformation of electricity into compressed air. Diabatic CAESs (D-CAESs) are already in use commercially as large-

⁷ Empirical Formula: $p_{max} = 0.18 * \text{depth of cavern roof in m}$ (Acht,2012)

⁸ The size of the biggest single cavern in Germany is in Etzel with 115 million m³ (Hannover, 2014). It uses methane as storage medium. The storage volume based on the given numbers suggest a cavern pressure of approx. 146 – 166 bar. If a cavern should also be usable as CAES, Haubrich (2007) suggest a maximum cavern volume of 500,000 m³ which corresponds to a storage volume of 77,500,000 m³.

⁹ Own calculations, based on Haubrich (2007) and Institute (2008), which suggest approx. 500 kg/s for a CAES with two caverns.

scale energy storage. Before the air enters the storage cavern it is highly compressed in a decoupled compression cycle of a gas turbine. Electricity bought on the spot market is used to power the compressors. To generate electricity, the compressed air is released with additional natural gas into the combustion chamber.

After the combustion, the compressed gas powers a turbine to generate electricity. Consequently, D-CAESs not only need electricity to operate but also natural gas (Hadjipaschalis, Poullikkas, & Efthimiou, 2009). But, due to the use of additional natural gas, D-CAESs have an electricity output to input ratio bigger than one. This means only approx. 0.7 MWh of stored electric energy is needed to discharge 1 MWh of electric energy.

Although the technology is mature, there are only two D-CAES facilities worldwide in operation. The major barrier to the implementation of further D-CAESs is the need for suitable geological sites and rather poor efficiencies. Salt caverns or depleted gas fields form the cheapest possibility to build a D-CAES (H. Chen et al., 2009). The simple design of the Huntorf D-CAES yields only an efficiency of approx. $\eta_{el-el}=42\%$.

This is why more advanced technological layouts of D-CAES have been developed. These concepts are based on a recuperator which uses the hot exhaust gas of the gas turbine to pre-heat the released compressed air from the cavern before entering an expander. All in all, this leads to an efficiency of approx. $\eta_{el-el}=55\%$ (Haubrich, 2007; Institute, 2008). But CAESs are not only suitable for intertemporal arbitrage on the electricity spot market they can also provide tertiary and secondary reserve (Eckroad & Gyuk, 2003). Though, there is one major drawback of the improved design: The usage of a recuperator which has to be heated before achieving higher loads leads to higher ramp-up times (20-35 min vs. 8-12 min) (Haubrich, 2007). This higher ramp-up time can have influence on the possibility of participation on the reserve energy market¹⁰, but has no influence of the possibility of intertemporal arbitrage, since the time needed to change charging or discharging rate is negligible compared to spot price period (1 h) (Barbour et al., 2012).

A technologically more advanced version of the D-CAES is the adiabatic CAES (AA-CAES), which in contrast to the diabatic CAES stores the emerging excessive heat during the compression process and re-uses this heat during the withdrawal. Consequently, no additional gas firing is needed and a higher round-trip efficiency is reached (Loisel, Mercier, Gatzert, Elms, & Petric, 2010). Though, an additional heat storage is needed, which leads to higher investment costs. Many scientific papers have been written about this topic but as of today no commercial AA-CAES plant has been built anywhere in the world (Loisel et al., 2010).

¹⁰ The impact of this drawback is explained in chapter 4.3 and relativized by Institute (2008).

This is the reason why this study will focus on the usage of a D-CAES plant with the basic data of the plant shown in from Haubrich (2007) and Institute (2008) (table 9, table 10).

Table 9: Technical specification of assumed CAES design – Part 1

Type	Value	Source / Base
Power compressor	300 MW [Sensitivity: $\pm 50\%$]	(Institute, 2008)
Power expander	255 MW	(Institute, 2008)
Power gas turbine	175 MW	(Institute, 2008)
Total power	430 MW [Sensitivity: $\pm 50\%$]	(Institute, 2008)
Max. charge rate	475 kg/s	(Institute, 2008)
Max. discharge rate	500 kg/s	(Haubrich, 2007; Institute, 2008)
p_{\min} (Turbine limitation)	60 bar	(Haubrich, 2007)
p_{\max} (Turbine limitation)	≤ 100 bar	(Haubrich, 2007)
Max. pressure difference Δp	40 bar ¹¹ , $\Delta p_{\text{average}} = 20$ bar	(Haubrich, 2007; Institute, 2008)

Table 10: Technical specification of assumed CAES design – Part 2

Type	Value	Sensitivity range	Source / Base
$P_{\text{el-comp}}/P_{\text{el-turb}}$	0.6966 ¹² kWh _{el-in} /kWh _{el-out}	[0.625-0.725]	Own calculations
$Q_{\text{gas}}/P_{\text{el-turb}}$	1.1158 ¹³ kWh _{gas-in} /kWh _{el-out}	[1.0 -1.25]	Own calculations
Roundtrip efficiency	0.55		Own calculations, (Barnes & Levine, 2011)
$\eta = (Q_{\text{gas}} + P_{\text{el-comp}})/P_{\text{el-turb}}$			
Cavern size	980,000 m ³ = 2 caverns ¹⁴	[500,000 m ³ –2,000,000 m ³]	(Haubrich, 2007)
Withdrawal time	55.7 h		Own calculations
Injection time	55.7 h		Own calculations

5.2.2 Gas cavern storage

In contrast to the usage of a cavern for compressed air, the pressure level of a gas cavern storage can be much higher. This is due to the fact that the gas arrives already pre-compressed at approx. 80–100 bar (FNB, 2014) so an additional compression to a level of 162 bar¹⁵ is less costly than a compression of air from ambient pressure to 80-100 bar. Moreover, the lower discharge and charge rates of gas cavern storages lead to lower stress in the salt layer, which is why higher pressure levels can be accepted (Haubrich, 2007).

¹¹ The maximum pressure difference Δp is limited due to stresses in the salt rock layer. Haubrich (2007) estimates the maximum allowed Δp to 40 bar, while $\Delta p = 20$ bar is estimated as optimal trade-off between cavern size and compressor size (higher Δp decreases cavern size but increases power consumption and size compressor). This is in line with the plant design of Institute (2008) which estimates a Δp in static view to 13 bar.

¹² This number explains how much electricity is used to generate 1 kWh of electricity output based on the plant design of Institute (2008). The number is slightly higher than assumed by (Haubrich, 2007) (0.697 vs. 0.625).

¹³ Amount of gas used in the gas turbine divided by the electricity output. Based on values from Institute (2008). Outcome is slightly lower than results from Haubrich (2007) (1.12 vs. 1.17).

¹⁴ Cavern size of Huntorf plant is 300,000 m³ (Haubrich, 2007; Raju, 2012), here the maximum size is assumed to be 500,000 m³. Max. operating storage pressure is 95 bar.

¹⁵ Maximum pressure limited due to assumed cavern height in section 5.1 (0.18 * 900 m = 162 bar).

The design of an injection and withdrawal site for a gas cavern storage is straightforward. The pre-compressed gas is compressed to a level of 162 bar. The withdrawn gas contains some moisture due to the storage process, which is why it has to be dried before it can be released into the pipeline network. After the dehumidifying process the gas has to be preheated to avoid too low temperatures after the expansion to pipeline-pressure-levels. Table 11 shows the technical specifications of an assumed natural gas storage. It is also based on two caverns, to be able to compare the performance of a gas storage with the performance of the previously defined CAES.

Table 11: Technical specification of assumed natural gas storage

Type	Value	Sensitivity range	Source / Base
Storage volume	155,000,000 m ³	[77,500,000 – 310,000,000]	(Haubrich, 2007)
Injection rate	150,000 m ³ /h	[75,000 – 300,000]	Own estimation
Withdrawal rate	300,000 m ³ /h	[150,000 – 600,000]	Own estimation
Injection loss	2%	[1% - 4%]	(Felix et al., 2013)
Withdrawal loss	2%	[1% - 4%]	(Felix et al., 2013)
Max. pressure	162 bar		Own calculation
Withdrawal time	21.5 days		Own calculation
Injection time	43 days		Own calculation

An important number is the injection and withdrawal loss. Both losses are assumed to be 2% of the gas amount each. This means that only 98% of the bought gas is injected into the cavern in order to power the compressor. Just like only 98% of the withdrawn gas arrives at the pipeline in order to power the pre-heating and dehumidifier unit. Real numbers on this losses are rare to find in literature which is why the value of Felix et al. (2013) is used.

5.2.3 CO₂ cavern storage

Salt caverns can also be used to store carbon dioxide. A possible business model could be the intertemporal arbitrage due to fluctuating EUA prices.

The transport of CO₂ is technically identical to the transport of natural gas due to the fact that same pipeline infrastructure and pressure levels can be used. CO₂ is preferably transported and stored in a supercritical state due to its high density in this state. The supercritical state is reached if the temperature and pressure exceeds 31° C and 7.4 MPa respectively (Eccles, Pratson, Newell, & Jackson, 2009). Which is why the same pipeline and storage values are assumed as for the gas cavern storage (for values see table 11). The only difference is that either additional gas or electricity is used for the operation of the compressor and pre-heater and dehumidifier.

Despite the possible usage of CO₂ as storage medium, as mentioned above, there are more favorable type of storages for CO₂. There are possibilities to sequester CO₂ indefinitely at a profit. Enhanced oil recovery (EOR) through the injection of CO₂ into existing oil fields is for

example a more economic approach. Due to the fact that one kilogram of sequestered CO₂ recovers approx. one to one quarter kilogram of extra oil, additional revenues through the sale of oil can be generated. The North Sea is expected to serve as an ideal location for EOR with CO₂, since Brent is lighter than WTI (thus easier to dissolve with CO₂) and the oil fields are more homogeneous than in the US. (Blunt, Fayers, & Orr, 1993). Further co-optimization can enhance the ratio of injected CO₂ to enhanced oil to be able to sequester even more CO₂ in the same oil field (Kovscek & Cakici, 2005).

It is expected that even without an increase in EUA that carbon capture and storage (CCS) technology will be in use in the upcoming years due to its economic benefit on the enhanced oil and gas recovery (van der Zwaan & Smekens, 2007). Another possibility is to use the sequestration of CO₂ in deep coal seams to produce coalbed methane (Krooss et al., 2002).

While there are several technical possible options for sequestration of carbon dioxide and even a few economic options, one has to keep in mind that there are still many gaps in the understanding of the CO₂ storage process in terms of leakage and dissolving of CO₂ in underground storages (Sean T. McCoy & Rubin, 2009).

5.2.4 Hydrogen cavern storage

There are world-wide three hydrogen storage sites in salt caverns in use¹⁶. Apart from that, there is a very important advantage of salt caverns compared to depleted oil and gas fields or aquifers as hydrogen storage: Salt acts inert, which is why there is no risk of a reaction of hydrogen with salt, while there is a significant chance of reaction with rock structures or microorganisms in other storage types (Acht, 2012; Ozarslan, 2012).

Though the usage of hydrogen as storage medium has a major drawback: At the same pressure level hydrogen has only approx. 30% of the caloric value of natural gas¹⁷. Consequently, the amount of storable energy with hydrogen is less than one third compared to methane. In contrast to methane, hydrogen is dissolvable in ground water which requires additional provisions to avoid any contact with water and hydrogen. This provision is typically the lowering of the overall pressure level to take the higher risk of leakage¹⁸ into account (Sørensen, 2007). Consequently, to store the same amount of energy in hydrogen instead of methane, a 5-6 times larger storage is needed. Thus the difficult storability compared to similar commodities decreases hydrogens economic viability (Budny, Madlener, & Hilgers, 2015). A possibility to increase the storable volume of hydrogen would be liquefaction. As Taylor, Alderson,

¹⁶ Teesside, UK; Clemens Dome, Moss Bluff and Spindletop in Texas, USA (Acht,2012; Ozarslan,2012).

¹⁷ Natural gas: assumed to be 100% methane with a calorific value of $H_{CH_4}= 35.883 \text{ MJ/m}^3$ (standard conditions) Hydrogen has calorific value of $H_{H_2}=10.783 \text{ MJ/m}^3$

¹⁸ The hydrogen molecule H₂ is smaller than the methane molecule CH₄, consequently higher risk of leakage. Sørensen (2007) suggests a maximum pressure of 50-100 bar, rather than 160-230 bar in his example cavern.

Kalyanam, Lyle, and Phillips (1986) states, the increased costs due to the technical challenge to liquefy hydrogen on a large-scale don't offset the gain through an increased capacity in the cavern.

On top of that, the design of the steel and sealing of the salt cavern has to be adapted in order to avoid the possibility of hydrogen embrittlement of steel (Ozarlan, 2012). Still, caverns are seen as the storage with the lowest cost for storing hydrogen compared to depleted gas fields, rock mined caverns and high-pressure tube storage (Taylor et al., 1986).

To increase the storability of hydrogen significantly, an additional step after the electrolysis can be included: Methanation. The methanation process merges hydrogen (H_2) with carbon dioxide (CO_2) to synthetic methane (CH_4), also called synthetic natural gas (SNG) (Budny et al., 2015).

The SNG can be injected into the gas grid. The overall efficiency from electricity to electricity of hydrogen compared to SNG is only slightly higher (approx. 40% vs. 36%) (Budny et al., 2015; Crotogino et al., 2010). Though, a paper by Budny et al. (2015) suggests that the direct sale of hydrogen to blend into the gas network is more economic viable than the methanation or the storage of hydrogen in a salt cavern to decouple production and sales.

This is why the storage of hydrogen is not incorporated into this study. The implementation is for further research, when large-scale electrolysis and fuel cells become more mature and affordable and a market for hydrogen beyond the chemical industry evolves.

5.3 Costs of storage

In the following section a cost estimation of a cavern storage and its components will be performed. Several sources of data will be compared and the most valid estimation chosen. Not only will the cost for the cavern itself be estimated but also the cost of a CAES, the cost to store natural gas and CO_2 .

5.2.1. Cavern costs

In order to assume the construction costs of salt caverns one has to keep in mind large variability of site characterization costs. The primary factor influencing the site characterization costs is the size of the area of review (Sean T. McCoy & Rubin, 2009). Major costs components are: (1) Site characterization costs; (2) Project capital costs (construction of the cavern – solution mining and drilling); and (3) Operation and Maintenance (O&M) costs.

Table 12: general assumptions on cavern dimensions

Maximum depth	1300 m	Working gas volume (V_N)	77.5 million m^3
Length of Cavern	400 m	Withdrawal rate (V_N)	175,000 m^3/h
Width (max.)	42 m	Injection rate (V_N)	87,500 m^3/h

Table 12 describes the technical assumptions on the dimensions of the selected cavern design. These assumptions are needed to estimate costs appropriately. A compressor is needed to increase the pressure of the medium before injecting it into the borehole. In reality, the compressor needs a higher pressure when the storage is nearly full, and less pressure if the storage is nearly empty. For simplification purpose, the pressure, and consequently the injection and withdrawal rate are assumed to be constant. The operating pressure and the pressure difference which the compressor has to generate depends on the usage of the storage site (CAES, etc.). Subsequently, those costs will be estimated for each application separately. The drilling process is straightforward, which is why oil and gas well equipment can be used (Acht, 2012). Based on the assumptions on site size and drilling depth (table 12), the estimated drilling costs including equipment is according to Bock et al. (2003) approximately €3.9 million (table 13), while Lukawski et al. (2014) put the cost of drilling at €1.7 million. The last source in table 13 estimates all relevant costs such as site characterization and injection piping at €8 million.

Table 13: Drilling and equipment costs based on several sources

Source	Cost in M€	Remarks
Bock et al. (2003)	3.87	Incl. equipment and permissions, converted from \$1998 to €2015
(Lukawski et al., 2014)	1.68	Only costs for oil/gas well
(Sean T. McCoy & Rubin, 2009)	7.51	Drilling and completion converted from \$2004 to €2015
(Sean T McCoy, 2008)	0.16	Site characterisation
	0.19	Equipping injection well
	<u>0.11</u>	O&M costs
	7.97	

It is hard to find reliable data on the exact construction costs of caverns (without additional equipment for gas storage or to use as CAES). Consequently, the table below (table 14) shows cost estimates of different sources. The cost estimates are scaled either by the assumed working gas volume (Sources no. 1–4) or by the assumed CAES size (Sources no. 5–6). There is a wide cost margin between €17 million and €100 million. Since some of the costs are total costs of ready-to-use gas storage caverns (including cushion gas – Sources 1–4), an assumption of cavern construction costs of €26 million for a 500,000 m³ cavern seems reasonable and is in line with source no 3, 5 and 6 of table 14. This is also in line with the previous estimations of drilling costs (table 13), which indicate drilling, equipment, injection piping and site characterization costs of approx. 8 million euros which would be 30% of the total construc-

¹⁹ The mined volume will never have perfect cylindrical shape, which is why the volume is less than expected from the length and width.

tion cost. Haubrich (2007) describes the price development of cavern mining as an unsteady process. There is certain base level of costs, independent of the cavern size due to site characterization and drilling costs, while the cost increases with size of the cavern gradually from this base level. This statement gives prove to previous findings.

Table 14: Cost of cavern construction based on different sources

No	Project / Source	Cost (in M€)	Remarks	Source
1	Katharina Kavernen	47.54	In total 12 caverns for gas storage incl. equipment for gas injection	(Schroeter, 2014)
2	Trainel Kaverne 4 Epe	100.75	One additional cavern incl. equipment for gas injection	(Trianel, 2010)
3	Storenergy Peckensen	29.21	Source states cost of one cavern without equipment as 25 M€	(Schröder, 2014)
4	EWE Jemgum	79.92	Eight caverns for 330 M€ including all equipment for gas injection	(Schürmeyer, 2013)
5	Drury et. al	28.32	Cavern only, price was given in \$2009/kW, converted to €2015 and 400 MW CAES assumed	(Drury et al., 2011)
6	CAES study California	17.00	Only cavern construction	(Institute, 2008)

To properly compare the overall revenues and costs of CAES, gas storage and CO₂ storage, the usage of two caverns is assumed. Subsequently, the investment costs for two caverns amounts to €52 million.

5.3.1 Gas storage costs

The cost for gas storages are the easiest to estimate since most of the data in table 14 is based is on recently realized gas cavern storages. Consequently, an estimate for a working gas cavern incl. cushion gas and all necessary infrastructure is the average of sources 1–4, which is approx. €65 million. The construction of a cavern costs about €26 million, consequently the additional costs for the possibility to store natural gas amounts to €39 million.

The most important cost component of gas storages, except for the cavern and cushion gas, is the compressor. The compressor has to compress from 80-100 bar to 162 bar, thus $\Delta p=82$ bar. The value of the cushion gas is approx. €0.34 million²⁰. If one estimates that the compressor accounts for roughly 70% of the remaining gas storage costs, the cost for the compressor train amounts to €7 million.

²⁰ Based on an natural gas price of 16€/MWh, caloric value of methane (35.833 MJ/m³) and a working gas storage volume of V_N=77,500,000 m³

Since two gas storage caverns are considered, the total additional costs amount to €78 million. The overall investment costs for cavern and gas injection facilities amounts to €130 million.

5.3.2 CO₂ storage costs

As described in subsection 5.2.3, the storage of CO₂ in caverns is from technical perspective nearly identical. This is why the same compressor trains and injection infrastructure can be used. Consequently, the cost of storage will be identical. This leads to additional costs for a CO₂ storage, excluding the cavern, of €39 million. Most importantly, switching from natural gas storage to CO₂ storage is possible at nearly no costs, since only the cushion gas has to be replaced (natural gas withdrawn and carbon dioxide injected). If no carbon dioxide source is nearby, pipeline connections have to be changed. That is why the switching process will be assumed to cost €3 million.

5.3.3 CAES costs

Table 15 shows the estimates for a compressed air energy storage based on different sources. The cost estimations of each source is transformed to €/kW and scaled to the chosen generator output (see also section 5.2.1). The overall costs differ from €193 million to €334 million. It is important to mention that sources 4-6 have the identical underlying source but interpret the data differently, which results in diverging costs.

Table 15: CAES cost estimations based on different sources

No	Source	Costs	€/kW	Remarks
1	(Haubrich, 2007)	250 M€	625 - 833	Compressor 250MW – Generator 300 - 400MW
2	(Institute, 2008)	193 M€	449 - 483	Compressor 288 - 300 MW – Generator 400 - 430 MW
3	(Drury et al., 2011)	334 M€	777	Drury's estimation is based on 81 MW compressor and 110 MW Generator – adjusted to 300 – 430 MW
4	(Keles, Genoese, et al., 2012)	237 M€	550	Based on 150 compressor and 300 MW generator –adjusted to 300 – 430 MW
5	(Gatzen, 2008)	258 M€	600 -750	See above
6	(Loisel et al., 2010)	297 M€	690	See above
	average	254 M€	592	

As explained in section 5.2.1, the CAES not only needs a compressor and cavern but also an expander and gas turbine. Consequently, the total investment costs are considerably higher than the storages for gas or carbon dioxide. The overall size of the CAES is developed according to the technical requirements of off-the-shelf gas turbines from major producers. The large compressor train, the heat recuperator and the expander or turbine are to a lesser extent mass products, which is why the economic performance is expected to improve. This can be achieved through using different designs or simplifications of technical designs (Baker,

2008). A reduction in investment costs by 15% by 2030 is a realistic assumption (Loisel et al., 2010).

Based on the estimates from table 15 the average cost for a 430 MW-sized CAES is approx. €254 million. The residual investment cost (after removing the cost for two caverns) is 202 million euros. The estimated share of the compressor costs is in the range of 10,6% (Institute, 2008) - 11% (Drury et al., 2011), in absolute terms €7.94 million.

Although the pressure levels for the usage of CAES are lower (but Δp similar) and the flow rate is higher, it is reasonable to assume that not an entire new compression train is needed if a change from a CAES facility to a gas storage facility occurs. This study assumes switching costs for the adjustment of the compression train to higher pressure levels in the range of 10 million euros. The change from a gas or CO₂ storage facility is the difference between initial CAES investment costs less cavern costs and compressor costs plus 10 million adjustment costs. The switching costs amounts to €158 million.

6. Economic storage model

The economic storage model incorporates the real options theory through the usage of random variations in revenue streams (Kroniger & Madlener, 2013). The price model over every commodity included in this simulation is partly based on a randomly distributed stochastic process. In order to account for the changing value of the storage due to varying prices, the optimal behavior of the storage operator is simulated for each price path. The overall estimated storage value is the mean of all storage valuations.

This study assumes the storage operator acts as a price taker and the market will not be influenced by any trades. Moreover, the market has incorporated all knowledge about the optimal usage of storage into the prevailing forward curve.

6.1 Basic structure

The optimal usage of a storage is mainly determined by the price spread of the stored medium at injection time $t-x$ and withdrawal time t of the medium. This process is economic if the spread is high enough to cover the marginal charge and discharge costs. The working principal of a storage can be seen as a spread option ($p_t - p_{t-x}$). The option is in the money, thus executed, if the spread achieves a positive value (Keles, Hartel, et al., 2012).

Optimal plant value can be described as the expected sum of the optimized returns from a series of spread options within the economic plant lifetime (Keles, Hartel, et al., 2012).

$$\max E \int_0^T e^{-rT} \left((p_t - c_{var})x_{spot}(t) - p_g(t) * x_g(t) - p_{CO_2}(t) * x_{CO_2}(t) \right) dt \quad (11)$$

This study will use a very basic LP (linear program) model to approximate the upper bound of revenues which can be generated with the usage of the storage. A LP tries to simulate complex nonlinear processes by breaking them apart into constituent linear processes. This approach is perfectly suited for complex optimization problems with multiple and competing decisions and constraints (Middleton & Bielicki, 2009).

For each simulated price path the optimal unit commitment is determined by the LP. The respective contribution margin, determined for each single simulated price path, is aggregated to an expected contribution margin by averaging. The difference between contribution margins of different price paths can be seen as real option value of the future scope of actions. The storage valuation is performed with a dual approach: (1) a realistic simulation with two weeks horizon and (2) an idealistic simulation with a horizon of 25 years (econ. timespan) as upper bound.

At first, the storage operator estimates the optimal dispatch strategy with the knowledge of future prices *a priori* for a time period of two weeks²¹. This approach is not unusual and ruled as good approximation (Connolly, Lund, Finn, Mathiesen, & Leahy, 2011; Drury et al., 2011; Keles, Hartel, et al., 2012; Sioshansi, Denholm, Jenkin, & Weiss, 2009). Every day the storage operator has foresight on the prices of the upcoming two weeks. Based on these market prices, the optimal unit commitment for the following day is determined. This unit commitment leads to a certain storage level at the end of the day. The calculated storage level will be used as basis for the following day to perform the unit commitment analysis once again. Consequently, the simulation of one price path with a length of 365 days needs 365 sub-simulations. If this linear program is expanded to 25 years and 500 price paths the computation time increases massively²². One run with only 5 price paths of this simulation takes with a decent desktop computer approx. 8 hours.

This is why a dual approach is needed. The second type of simulation is conducted with a further simplified model. The simulation is carried out with perfect foresight on prices. Subsequently, the number of sub-simulations decreases from t (number of days in dataset) to 1. The idealistic simulation runs only one time for every price path. Since the operator knows all future prices in advance, the number of calculated data points for each price path is 14-times lower.

The usage of a two-week optimization horizon allows for both intra- and inter-day arbitrage opportunities, including greater charging during weekend because hourly electricity

²¹ Connolly et al. (2011) and Keles et al. (2012b) even use 12 month perfect foresight on market prices.

²² In total $25 \cdot 365 \cdot 14$ calculated data points per price path (with daily price).

prices often tend to be lower than during the week. An optimization over a two-week period accounts for the fact that a storage operator would not have realistically a foresight on prices many weeks in the future.

The following equations describe a general heuristic approach to estimate the optimal decision with perfect foresight on prices in the upcoming two weeks. Subsections 6.2–6.5 describe necessary changes and extensions of the general model to fit on the specific use case (CAES, gas storage, CO₂-storage).

Equation (12) describes the general objective function²³ with the aim of finding the optimal storage usage. The aim is to maximize the spread between charging and discharging prices, allowing for operation and maintenance costs of compressor and turbine as well as costs for supplemental media.

$$\begin{aligned} Z(i) = \max \sum_{t=1}^T & x_{out}(t)P_{medium}(t) - x_{in}(t)P_{medium}(t) - x_{in}(t)P_{helpin}(t)UF_1 \\ & - x_{out}(t)P_{helpout}(t)UF_2 - x_{out}(t)c_{turb} - x_{in}(t)c_{comp} \end{aligned} \quad (12)$$

The general idea is to maximize the spread between revenue from the withdrawal of the stored medium and the injection of the stored medium over time. The cost of the injected medium and the cost for injection and withdrawal is subtracted from the revenue generated from the withdrawal.

The constraints are similarly constructed for all storage media. The main constraints are limits for injection & withdrawal rates (eqs. (16) and (17)) and storage size (equation (15)). Moreover, the storage balance (eq. (14)) is needed to account for the losses occurring in storage process. It is important to note that for simplicity reasons the operation and maintenance cost (O&M) are assumed to be constant over the lifetime and dependent on the amount of stored media injection or withdrawn over time (€/MWh). On top of that, the maximum injection and withdrawal rates are assumed to be constant and the minimum compressor and turbine power is zero.²⁴

Table 16: Constraints of the general LP

$$l(0) = l(T) = 0 \quad (13)$$

$$l(t) = x_{in}(t) * EFF_{in} - x_{out}(t) * EFF_{out} + l(t - 1) \quad (14)$$

$$0 \leq l(t) \leq l_{max} \quad (15)$$

²³ General objective function is simplified for a better appearance and readability without consideration of discounting of revenue streams and only limited foresight. The complete model can be found in the digital appendix.

²⁴ Further details on this topic can be found in section 6.5.

$$p_{comp-min} \leq x_{in}(t) \leq p_{comp-max} \quad (16)$$

$$p_{turb-min} \leq x_{out}(t) \leq p_{turb-max} \quad (17)$$

Table 17 explains all variables used in eqs. (12) - (17).

Table 17: Definition of variables of general storage model

$x_{out}(t)$	Amount of medium sold	$x_{in}(t)$	Amount of medium stored
$P_{helpin}(t)$	Price of medium used to inject at time t	$P_{medium}(t)$	Price of medium at time t
$P_{helpout}(t)$	Price of medium to withdraw at time t	UF_1	Utility factor 1
EFF_{in}	Efficiency factor of injection process	UF_2	Utility factor 2
EFF_{out}	Emission factor of withdrawal process	c_{comp}	Operating costs compressor
$l(t)$	Storage level at time t	c_{turb}	Operating costs turbine
$p_{comp-min}$	Minimum power of compressor	I_{max}	Maximum storage level
$p_{comp-max}$	Maximum power of compressor	$P_{turb-min}$	Maximum power of turbine
$P_{turb-max}$	Minimum power of turbine		

The formulas given in (32)-(38) have to be seen as general concept and are in principle applicable for both approaches. The integral (31) is the theoretical description of the optimization problem but not solvable in a closed form. This is why a linear program is developed to approximate the upper bound of revenues which can be generated with the usage of the storage.

After the Monte Carlo simulation of the most economic unit commitment over a time period of 25 years and 500 price paths, the results are post-processed. The yearly return of every price path is first discounted with a weighted discount rate. Afterwards the yearly discounted results of each price path is summed up. Finally, the mean storage value of all price paths is calculated (eq. (18)).

$$V_{storage} = \frac{1}{N} * \sum_{i=1}^N \sum_{\tau=1}^T \frac{Z(i, \tau)}{(1+r)^\tau} \quad (18)$$

To calculate a suitable discount rate as basis for the present value of the storage site the Weighted Average Cost of Capital (WACC) method will be applied. This approach calculates an average discount rate based on equity and debt interest rates (Ross, Westerfield, & Jordan, 2008). Based on an in-depth analysis of reasonable equity and debt interest rates by Fraunhofer (2013), the following discount rate is estimated:

Table 18: Discount rate calculation based on WACC (Fraunhofer, 2013; Ross et al., 2008)

Equity ratio	S_{equity}	40%
Debt ratio	S_{debt}	60%
Interest rate on equity (nominal)	$r_{equit,nom}$	13.5%
Interest rate on debt (nominal)	$r_{debt,nom}$	6%
WACC _{nominal}	$WACC_{nom}$	9%

Expected inflation rate	z_{infl}	2%
Discount rate $WACC_{real}$ ²⁵	r	6.9%
Economic lifetime	T	25 a

The simulated spot prices represent real prices since price level is assumed to be constant over the time period of 25 years. This is why nominal interest rates have to be adjusted by the inflation rate to represent real interest rates. In order to secure an easily calculable discount rate, a constant inflation rate over the upcoming 25 years of 2% is assumed. This is a clear simplification of the variation of inflation rates in the real world, but common practice in academic literature (Fraunhofer, 2013). The resulting discount rate is $r=6.9\%$ p.a.

6.2 Model details for CAES

Equation (19) describes the objective function of the CAES storage model. The most important difference between the general model and the CAES model is the inclusion of the heat rate ($EFF_{st-elect}$), which is defined as the usage of natural gas for every sold MWh of electricity.

$$Z(i) = \max \sum_{t=1}^T x_{out}(t) * P_{elect}(t) - x_{in}(t) * P_{elect}(t) - x_{out}(t)c_{turb} - x_{in}(t)c_{comp} - x_{out}(t) * EFF_{st-elect} * [P_{gas}(t) * + P_{co2}(t) * EF] \quad (19)$$

Table 19 describes the variables of the CAES storage model for the base variant. In section 7.1 further variants are defined to test the sensitivity of the value of the CAES with changing parameters. It is important to note that the assumed parameter values differ significantly from source to source. The efficiency values are based on the CAES design presented in Institute (2008). The O&M cost of turbine and compressor are assumed to be 1 €/MWh, respectively. This is in line with Gatzen (2008), while according to Lund, Salgi, Elmegaard, and Andersen (2009), operating costs of compressors are approx. 2.3€/MWh and for the turbine approx. 2.7 €/MWh.

Table 19: Definition of CAES storage model variables

Variable	Description	Value (base variant)
x_{out}	Amount of electricity sold	-
x_{in}	Amount of electricity bought	-
P_{CO2}	CO ₂ price path	-
P_{elect}	Electricity price path	-
P_{gas}	Natural gas price path	-

²⁵ $WACC_{real} = \frac{(1+r_{equity,nom}) * s_{equity}}{(1+z_{infl})} + \frac{(1+r_{debt,nom}) * s_{debt}}{(1+z_{infl})}$

$EFF_{st-elect}$	Heat rate (usage of natural gas for every sold unit of electricity)	1.1158 (MWh _{gas} /MWh _{elect})
EF	Emission factor natural gas	0.2 (t _{CO2} /MWh _{gas})
c_{turb}	Operating and maintenance costs turbine	1 (€MWh _{elect})
c_{comp}	Operating and maintenance costs compressor	1 (€MWh _{elect})
EFF_{in}	Compressed air energy factor (amount of electricity needed to sell one unit of electricity) – used in constraints party (equation (14))	1/0.6966 (MWh _{elect-in} /MWh _{elect-out})

6.3 Model details for gas storage

The objective function of the gas storage model (eq. (20)) is nearly identical with the general objective function (eq. (13)). Table 20 shows the explanation and values of the newly introduced variables.

$$Z(i) = \max \sum_{t=1}^T x_{out}(t)P_{gas}(t) - x_{in}(t)P_{gas}(t) - x_{out}(t)EFF_{st-gas}P_{co2}(t)EF - x_{in}(t)EFF_{cs-co2}P_{co2}(t)EF - x_{out}(t)c_{turb} - x_{in}(t)c_{comp} \quad (20)$$

Table 20: Definition of gas storage model variables

Variable	Description	Value
x_{out}	Amount of natural gas sold	-
x_{in}	Amount of natural gas bought	-
EFF_{st-gas}	Efficiency of re-injection into the gas pipeline (usage of NG to preheat and dehumidify released NG)	0.98
EFF_{cs-co2}	Efficiency of compressor (usage of NG to compress NG to storage pressure)	0.98
c_{turb}	Operating and maintenance costs turbine	0.1 (€MWh)
c_{comp}	Operating and maintenance costs compressor	0.1 (€MWh)

6.4 Model details for CO₂ storage

The objective function of the CO₂ storage (eq. (21)) has been modified compared to the general objective function (eq. (13)) due to the fact that a CO₂ storage generates revenue with the injection of CO₂ into the storage (avoided EUA) and generates costs when it releases CO₂. Consequently, the algebraic signs have changed. Moreover, the compression, preheating and dehumidification are assumed to operate on natural gas. This is why for every tonne of injected carbon dioxide a certain amount of natural gas is needed, which in turn emits again some carbon dioxide.

$$Z(i) = \max \sum_{t=1}^T x_{in}(t) * P_{CO2}(t) - x_{out}(t) * P_{CO2}(t) - x_{out}(t) * EFF_{st-co2} * [P_{gas}(t) * + P_{co2}(t) * EF] - x_{in}(t) * EFF_{cs-co2} * [P_{gas}(t) + P_{CO2}(t) * EF] - x_{out}(t) * c_{turb} - x_{in}(t) * c_{comp} \quad (21)$$

The constraints of the CO₂ storage model are similar to equation (13) - (17) except for the fact that no losses of the CO₂ occur during injection and withdrawal process. Consequently, EFF_{in} and EFF_{out} are assumed to equal 1. Table 21 shows the explanation and values of the newly introduced variables.

Table 21: Definition of CO₂ storage model variables

Variable	Description	Value
x_{out}	Released carbon dioxide	-
x_{in}	Stored carbon dioxide	-
EFF_{st-co_2}	Efficiency storage-turbine (usage of NG to preheat and dehumidify CO ₂)	0.0503 (MWh _{gas} /tCO ₂)
EFF_{cs-co_2}	Efficiency compressor-storage (usage of NG to compress CO ₂)	0.1007 (MWh _{gas} /tCO ₂)
c_{turb}	Operating and maintenance costs turbine	0.1 (€/MWh)
c_{comp}	Operating and maintenance costs compressor	0.1 (€/MWh)

6.5 Limitations

The storage model assumes that the necessary time to change from charging to discharging is negligible compared to the smallest traded timeslot on the spot market. This is not totally true, since there is some time necessary to ramp up or ramp down the compressor or turbine. Haubrich (2007) describes ramping times for his CAES concept of approx. 10-15 min. Consequently, the simplification to neglect the necessary time to change from charging to discharging is reasonable. This is in line with assumptions of Barbour et al. (2012).

The storage is able to operate 364 days a year. The limitation to 364 days is for simplicity chosen, since 364 is dividable by 7. Subsequently, the weekly pattern is easier to simulate. In the real world one should assume an availability lower than 100%, more in the range of 90-95% per year.

The model assumes the minimum compressor and turbine power to be zero, while real compressors and turbines have a minimum load in the range of 20-40% of the maximum load. This simplification allows a faster simulation since no additional “on-off”-state of the compressor and turbine has to be included into the model.

One of the biggest limitations of this optimization approach is the perfect foresight on hourly energy prices. A real operator has no perfect foresight and might not be able to capture the entire value of a storage. Especially for the hourly electricity spot market even two weeks foresight (limited foresight alternative) is rather long. Consequently, all results should be seen as an upper revenue bound. This approach is not unusual and Sioshansi et al. (2009) analyzed the impact of a more realistic approach with an operator who decides the operation mode (inject, withdrawal, do nothing) based on the previous two weeks' hourly prices. After the opera-

tion mode decision, the value of the trade was estimated with the real prices. The two-week Backcasting approach captured about 85% of the perfect foresight estimation and can be seen as lower bound (Sioshansi et al., 2009). Practitioners have more advanced price model /estimation tools based on several fundamental data, which allows them to estimate future prices more accurately than with rudimental historic prices. Subsequently, a perfect foresight approach for a limited time period (e.g. two-weeks) is a legitimate simplification.

Deployment of energy storages on large-scale would, in the long run, influence market prices of the stored medium and smoothen the load and price pattern at gas, CO₂ or electricity markets, respectively, by reducing peak prices and increasing off-peak prices. As described earlier, the model assumes that the operator is a price taker and does not influence prices due to the fact that the overall capacity is marginal compared to the entire market capacity (see also Sioshansi et al. (2009)).

The storage model assumes constant injection and withdrawal rates, while a real cavern storage would have lower injection rates when the storage is nearly full and lower withdrawal rates when the storage is nearly empty. In contrast to Thompson (2012), no level and pressure dependent injection and withdrawal rates are integrated, due to performance considerations.

7. Results

The following section is subdivided into three sections. First, all variants (sensitivities) are defined and summarized in a table. Second, the simulation results of the base case and the additional CO₂ price regimes are presented. Moreover, the profitability of each investment is assessed. Finally, all remaining variants are analyzed and presented.

7.1 Variants definition

The base variant, as described in the previous section, will be simulated with limited foresight and perfect foresight. In order to map the effect of a limited amount of storage parameters on the storage valuation with a reasonable computation time, the simulation of sensitivities is carried out with perfect foresight on prices. The simulation results of the base case show that the usage of carbon dioxide as a medium creates no revenue with intertemporal arbitrage, which is why the sensitivity analysis of the CO₂ storage will be limited only to reduced O&M costs. Table 22 shows a range of parameter values and the associated variants.

Table 22: Definition of variants to calculate sensitivities

O&M	Natural Gas			Electricity			CO ₂
	Base	N1.1	N1.2	Base	E1.1	E1.2	C1.1
Sensitivity		-50%	+100%		-50%	+100%	-50%
c _{comp}	0.1	0.05	0.2	1	0.5	2	0.05

c_{turb}	0.1	0.05	0.2			1	0.5	2		0.05
Flow rates	Base	N2.1	N2.2	N2.3	N2.4	Base	E2.1	E2.2	E2.3	E2.4
Sensitivity	MWh	-50%	+100%			MWh	-50%	+50%		
$p_{comp-max}$	34,680	17,340	69,360	69,360	34,680	300	150	450	450	300
$p_{turb-max}$	69,360	34,680	138,720	34,680	34,680	430	215	645	215	215
Flow rates	N2.5	N2.6	N2.7	N2.8		E2.5	E2.6	E2.7	E2.8	
$p_{comp-max}$	69,360	17,340	34,680	17,340		450	150	300	150	
$p_{turb-max}$	69,360	69,360	138,720	138,720		430	430	645	645	
Storage size	Base	N3.1	N3.2			Base	E3.1	E3.2		
Sensitivity	GWh	-50%	+100%				-50%	+100%		
I_{max}	1,545	772.5	3,090			23,972	11,986	47,944		
Efficiency	Base	N4.1	N4.2			Base	E4.1	E4.2	E4.3	E4.4
UF_1	0.98	0.96	0.99			1.1158	1.0	1.0	1.25	1.25
UF_2	0.98	0.96	0.99			0.6966	0.625	0.725	0.625	0.725

7.2 Base variant

The following subsection describes the simulation results based on technical and cost assumptions from section 5.

7.2.1 Natural gas storage

Figure 19 describes the fluctuating revenues of ten different price paths. Due to revolving negative revenues in certain years, a strong seasonal pattern becomes obvious. This means that the main share of the revenue, generated by the gas storage, is seasonal or even long-term trading.

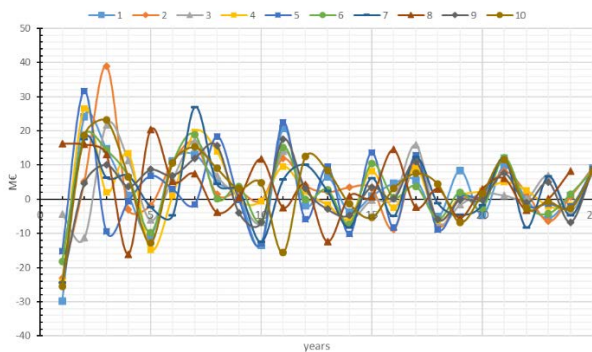


Figure 19: Fluctuating discounted gas storage revenues depend on price paths

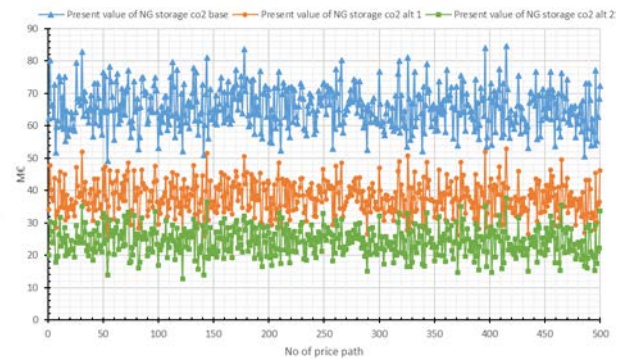


Figure 20: Impact of different CO2 price levels on the economics of the gas storage

Figure 20 shows the present value of all simulated gas price path for the base price level of CO_2 and for the increased price regimes (alt 1 & alt 2). The total present value of the high price regime (alt 2) is approx. 20 million euros, while the base regime has an average present value of approx. 66 million euros. The negative impact of higher CO_2 prices on the profitability of the gas storage is due to the gas consumption and consequently CO_2 emission to inject and withdrawal natural gas.

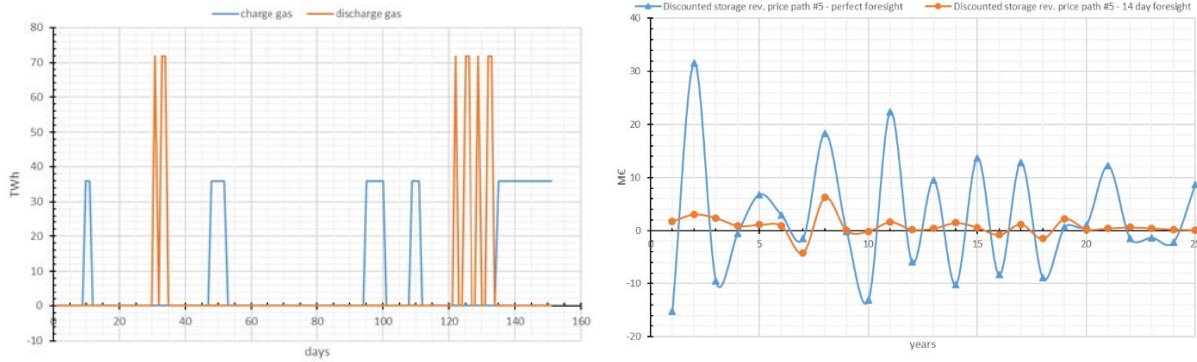


Figure 21: Excerpt of charge and discharge pattern of simulation path 5 with perfect foresight

Figure 22: Comparison of natural gas storage revenue with perfect foresight and limited foresight

Figure 21 describes the discharge and charge pattern of the natural gas storage with perfect foresight. As stated previously, the storage operator is rather operating on the long-term scale than on a spot market. This is due to the limited price spreads in the natural gas price paths.

A huge difference between the discounted yearly revenue of the gas storage with perfect foresight and limited foresight is shown in figure 22 and figure 23. Although only one price path is shown in this figure, the overall average earnings with limited foresight is about 22 million euros, while the storage value with perfect foresight is approx. 66 million euros (see also figure 23). Again, the usage of gas storages for long-term trading becomes obvious. Due to the fact that gas prices are far less volatile than electricity prices, a reasonable foresight period would probably be longer than 14 days.

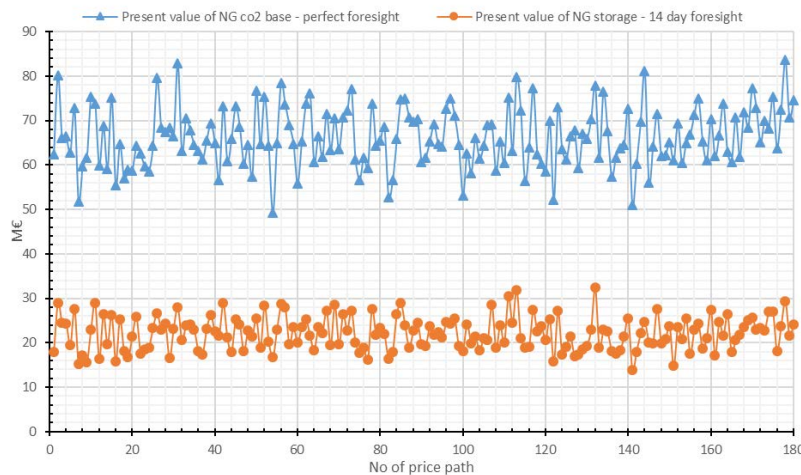


Figure 23: Present value of natural gas storage with perfect and limited foresight for each price path

Even with perfect foresight, the sum of average discounted revenue is not enough to cover the investment costs. In section 5.3.2 the investment costs of gas storage facility including equipment and caverns is estimated to be 130 million euros. Consequently, the discounted revenue over 25 years covers only half of the investment costs. Based on these findings, an investor would not invest into a gas cavern storage. With limited foresight the overall revenue is less than 20% of the total investment value. Only the lower bound of the sensitivity range (50% less storage construction costs than expected), becomes the investment reasonable.

7.2.2 CAES

In contrast to the natural gas storage, figure 24 shows rather constant revenues. On top of that, the impact of higher CO₂ prices on the economics of the CAES is significantly smaller than the impact of higher CO₂ prices on the gas storage. The summed average discounted earnings amounts to approx. €52.5 million in the base case and €32.4 million respectively €18.6 million for the first and second alternative regime.

Figure 25 emphasizes the above mentioned findings. The overall variances between price paths is rather small and the impact of higher CO₂ prices with about 20% less revenue in the worst case, still manageable. However, the present value of the CAES in the base case is not enough to cover the investment costs of approx. €254 million. Just as the natural gas storage, only with a significant reduction of the construction costs by 50%, the investment in a CAES turns out to be profitable.

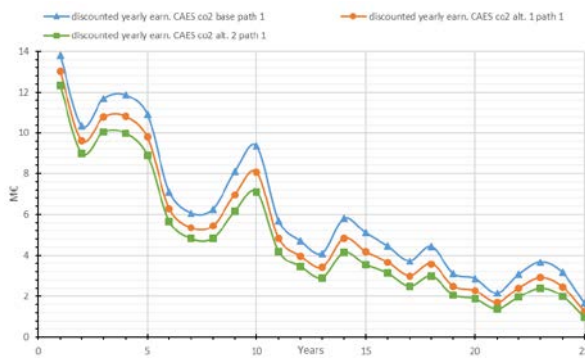


Figure 24: Discounted revenues of CAES dependent on CO₂ path

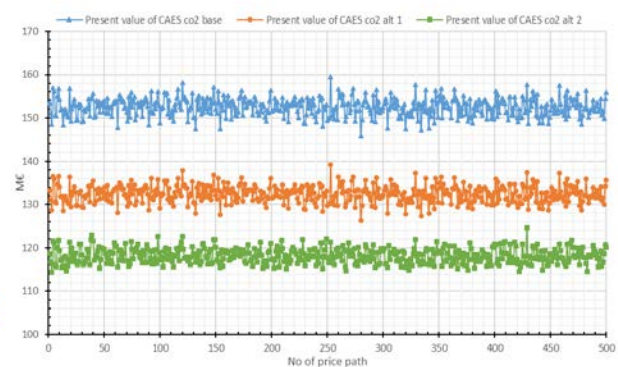


Figure 25: Impact of different CO₂ price levels on the economics of the CAES

The charge and discharge pattern shown in Figure 26 has a significantly higher frequency compared with the results of the gas storage simulation. Moreover, the CAES operator decides hourly, while the natural gas storage operator decides daily, due to the lack of a liquid hourly natural gas market.

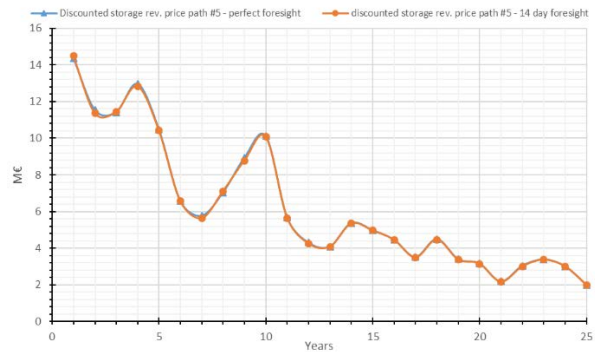
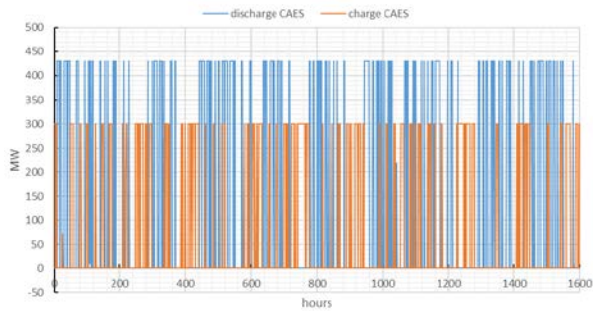


Figure 26: Excerpt of charge and discharge pattern of simulation path 5 with perfect foresight

Figure 27: Comparison of CAES revenue with perfect foresight and limited foresight

The comparison of the discounted CAES revenues with perfect foresight and limited foresight has only limited significance due to the extremely long simulation time of the storage model with limited foresight. This is why only five price paths are calculated with limited foresight. Interestingly, the difference in storage value between a 14-day foresight and perfect foresight is negligible. The average earnings with limited foresight (based on solely 5 price paths) is €152.4598 million, while the CAES value with perfect foresight amounts to €152.4768 million. These findings are much better than the estimates of Sioshansi, Denholm, and Jenkin (2011).

7.2.3 CO₂ storage

As described in section 7.1, the CO₂ storage model does not generate any revenues because of the too small volatility spread in conjunction with rising CO₂ prices over time. This is why only four price paths out of 500 generate a profit for the base CO₂ price case. This profit is marginal (less than €10,000 in total). The height of the profit does not significantly change with the implementation of the sensitivity variant. Consequently, EUA are not suitable for intertemporal arbitrage.

7.3 Sensitivity analysis

As defined in section 7.1, in the following, the flow rates, storage size, efficiency and O&M costs are varied.

7.3.1 Natural gas storage

The increase of O&M costs by 100% has a rather small impact on the overall present value. The present value decreases by approx. 6% from €66 million to €62 million. On the other hand, the decrease of the O&M costs by 50% increases the present value to €68 million. As figure 28 shows, the impact of different flow rates on the profitability of the gas storage is enormous. It turns out strategy N2.4 seems to be the most profitable. Variant N2.4 decreases the withdrawal rate by 50%, while the injection rate stays constant. This leads to equal injec-

tion and withdrawal rates. This strategy leads to a present value of 105 million euros, which is 60% more than the base case.

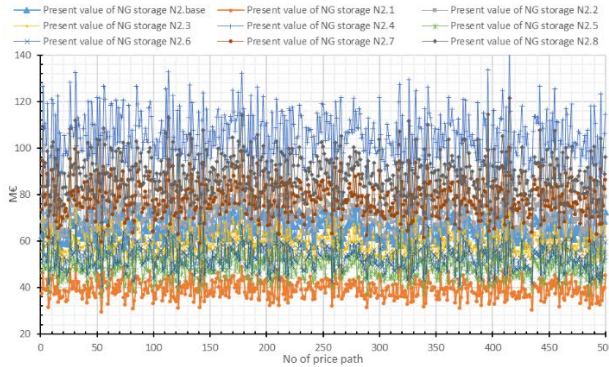


Figure 28: Impact of different flow rates on the present value of the natural gas storage

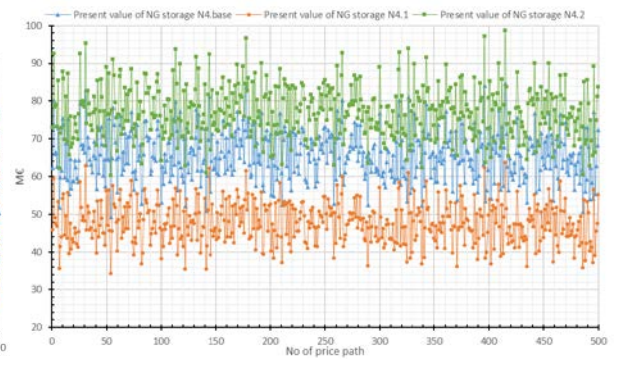


Figure 29: Impact of the change in charging and discharging efficiency on the present value of the natural gas storage

A 100% increase of storage size leads to a 16% increase of the present value, while a reduction by 50% results in 30% reduction in revenue. This can be interpreted as a sign that the storage size seems pretty well chosen (Sensitivity N3 – N3.2).

In contrast to the limited impact of changing O&M costs, the increase of charging and discharging efficiency leads to significantly higher revenues. A rise of 0.01 efficiency points leads to nearly 20% higher revenues, while a reduction by 0.02 efficiency points decreases the revenue by 20% (see figure 29).

All in all, an optimization of the injection and withdrawal rate simultaneously with the enhancement of the charge and discharge efficiencies could lead to high enough revenues to pass the break-even point.

7.3.2 CAES

The reduction of the O&M costs by 50% leads only to a 6% increase of the average earnings, while a 100% increase of the O&M costs lead to a 10% decrease of the average earnings (variants E1 – E1.2).

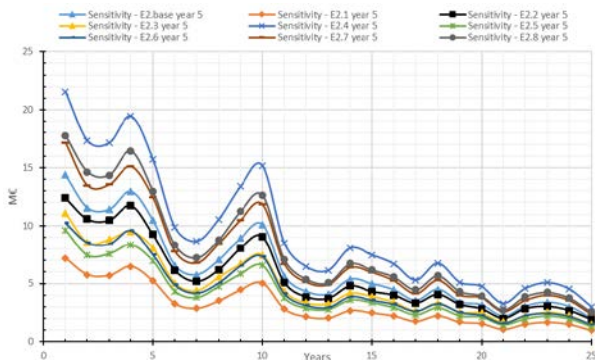


Figure 30: Impact of different flow rates on the discounted revenue of the CAES

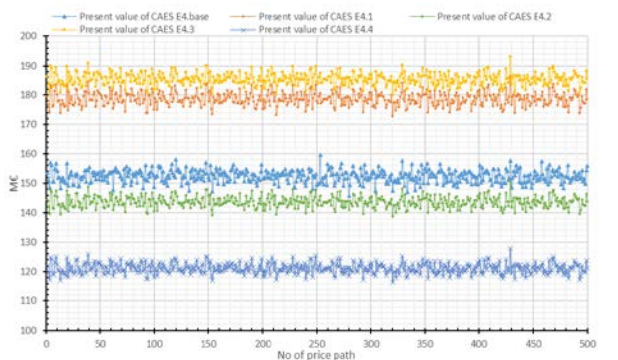


Figure 31: Impact of the change in charging and discharging efficiencies on the present value of the CAES

The impact of the adjustment of the flow rates, as shown in figure 30 is very significant. The best case (E2.4) increases the earnings by 50%, while the worst case leads to a revenue reduction of 50%. The best case is, once again, the case with equal injection and withdrawal rates.

Figure 31 shows the impact of different charging and discharging efficiencies on the present value of the CAES. E4.3 and E4.1 increase the storage value by 22% and 17% respectively, while E4.4 reduces the storage value by roughly 20%. Consequently, the most efficient improvements to increase the present value of the CAES are the adjustment of the flow rates and the enhancement of the injection and withdrawal efficiency.

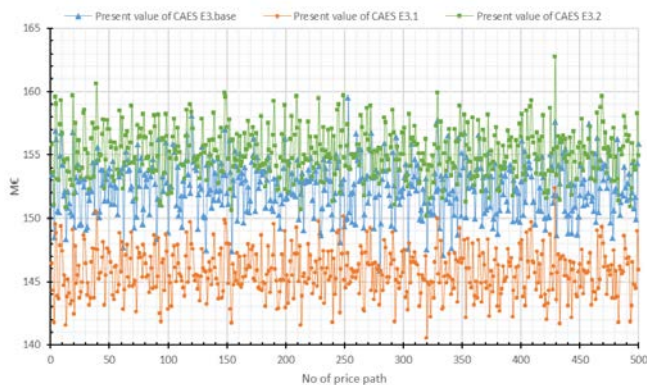


Figure 32: Impact of different storage sizes on the present value.

The impact of different storage sizes on the overall present value is very small. This can be the result of a high cycling rate and enough price volatility to trade nearly hourly. On the one hand, figure 32 shows an increase of present value by 2% when the storage size increases by 100%. On the other hand, a reduction of the storage size by 50% leads to a present value reduction of only 4.5%. This can be interpreted as a sign to decrease the storage size in order to save construction costs.

8. Conclusion

The purpose of this study was to create a multi-purpose storage model to evaluate the most economic storage medium for one specific cavern storage. The uniqueness of the approach is the assessment of the most suitable storage medium for one specific storage, while most academic literature deals with the search for the most suitable storage for one specific medium.

After an introduction into the applied theory, datasets and most important literature, the status quo and expected development of possible storage media such as electricity, natural gas, carbon dioxide and hydrogen is analysed. This analysis is performed with fundamental market data in order to map the dependencies and correlation of those storage media.

Because of the non-existent market and infrastructure for hydrogen and the rather difficult storability, hydrogen is excluded as storage medium. With the historical price paths of the

remaining candidates, extensive price models are created. The historical prices are decomposed into a deterministic and a stochastic part. In order to account for the relatively long simulation timeframe (25 years), the deterministic part of the prices is reproduced with rather complex sinusoidal (electricity and natural gas) or power functions instead of a constant drift term as used in many academic papers. The mathematically identified patterns are in line with previous fundamental observations and findings. The stochastic part is modelled with a Markov regime switching approach (with different numbers of regimes depending on the medium), which is especially suitable for price series with a high frequency of spikes and drops. Due to the stochastic price process, for every storage medium 500 price paths are calculated. These price paths are solved successively in the storage model in order to treat the storage as a real option.

After the analysis of potential storage sites and the identification of the most important technical properties, the potential costs are estimated. The cost assessment turns out to be rather complicated because of the inherent data and wide differences in costs. Especially the estimation of CAES costs is not very sound, due to the fact that there are only two existing CAES in the world.

In contrast to the price models, which were rather complex, the chosen storage model is designed as a simple linear program to be able to adjust the restrictions and objective function easily for every storage medium. A linear program has no issues with numerical traceability or heavily simplifying assumptions to reach solvability. The major drawback is a very high computation time due to the Monte Carlo simulation of 500 price paths. This is why only a part of the simulation is conducted with limited foresight (the operator can perfectly predict the prices of the upcoming two weeks). All other simulations are performed with perfect foresight on future prices.

Interestingly, it turns out that the CAES valuation with limited foresight is nearly identical to the storage value with perfect foresight. This is due to the fact that the CAES is operating hourly and has a very high cycling rate and only limited storage capacity (approx. 12h). By contrast, the value of the natural gas storage with limited foresight accounts only for 20% of the value of the storage with perfect foresight. This is due to the fact that natural gas is only traded daily and the daily and weekly spreads are rather small. Consequently, with perfect foresight, the operator trades mainly seasonally, while with limited foresight only short-term trades are possible.

Most importantly, the simulation results suggest that neither the natural gas storage, nor the CAES generate enough revenue to reach the break-even within 25 years. Only if the investment costs are significantly reduced (by 40-50%) will the investment be profitable. The CO₂

storage turns out to be unprofitable, due to the fact that the price volatility is too small and covers the marginal costs and the constantly increasing CO₂ price makes seasonal trading impossible.

The definition of several variants yields interesting results concerning the sensitivity of the storage value. A stronger increase in CO₂ prices leads to heavily decreasing natural gas storage revenues, while the CAES is only slightly influenced. Both storage media benefit from increasing charging and discharging efficiencies as well as the alignment of the injection rate with the withdrawal rate. If both parameters are adjusted, the natural gas storage and the CAES are profitable.

All in all, the solid storage model based on complex price paths suggests that no storage application should be implemented at this point in time. However, some additional revenue streams, which are addressed in the following subsection could improve the profitability significantly.

Most of the academic literature dealing with the potential of compressed air energy storage finds that solely wholesale price arbitrage is not enough to retrieve the high initial investment costs with an acceptable internal rate of return (Loisel et al., 2010). That's why often secondary and tertiary reserves provision is seen as a second source of income. The current system of secondary and tertiary reserve provision in the German electricity market is seen as not sustainable in the long run (Haubrich, 2007). This is due to the fact that the increasing share of RE stresses the profitability of existing fossil-fired power plants. If more and more fossil-fired power plants are phased out, less secondary and tertiary reserve can be provided. This is why a political discussion about capacity compensation to prevent fossil-fired power plants to be phased out, a so-called capacity market, is emerging. Due to the expected regulatory changes a simulation of future reserve market prices for the next 25 years is not useful. Further research has to be done in this field when the outcome of the political discussion emerges.

The costs of a gas cavern storage could be reduced with the substitution of the cushion gas with carbon dioxide. Which could on the one hand decrease the initial investment costs (no costly natural gas cushion needed) and on the other hand enhance available storage volume. Due to the fact that carbon dioxide is way more compressible, less cushion gas is needed to exploit the range of pressure Δp , and consequently significantly larger quantities of working gas can be stored. The effect of mixing of CO₂ with methane is still questionable and has to be tested in reality. Models predict limited mixing in gas reservoirs with large vertical extension (caverns) because of the higher density of CO₂, but it is still questionable how high cycling rates influence the mixing of CO₂ and methane (Oldenburg, 2003).

The usage of hydrogen as a storage medium is left for further research. Additional research is to a lesser extent needed from a technical perspective but more from an economic perspective. As described in section 3.4, there exists no transparent and liquid hydrogen market, which is why neither operation in terms of intertemporal arbitrage is possible nor are large-scale electrolysers available off the shelf. If a more mature hydrogen market emerges, the storage model should be extended. An extension of the storage model could be a trading pattern between daily off-peak and peak electricity contracts. This trade would only be conducted if the price difference between the off-peak and peak contract would be high enough to cover the marginal charge and discharge costs. The implementation of a switching model was already conducted, but due to the outcome that neither the CAES nor the natural gas storage are profitable, the switching model had no function. For further research, a deeper integration of a switching model should be addressed.

References

- Acht, A. (2012). Gasspeicher-Technologie und Herausforderungen. Retrieved from http://www.leuphana.de/fileadmin/user_upload/portale/inkubator/veranstaltungen/Praesentationen_Energieforum/Workshop_Windgas_Acht.pdf
- Adner, R., & Levinthal, D. A. (2004). What is not a real option: Considering boundaries for the application of real options to business strategy. *Academy of management review*, 29(1), 74-85.
- Baker, J. (2008). New technology and possible advances in energy storage. *Energy Policy*, 36(12), 4368-4373.
- Barbour, E., Wilson, I. G., Bryden, I. G., McGregor, P. G., Mulheran, P. A., & Hall, P. J. (2012). Towards an objective method to compare energy storage technologies: development and validation of a model to determine the upper boundary of revenue available from electrical price arbitrage. *Energy & Environmental Science*, 5(1), 5425-5436.
- Barnes, F. S., & Levine, J. G. (2011). *Large energy storage systems handbook*: CRC Press.
- Benz, E., & Trück, S. (2009). Modeling the price dynamics of CO₂ emission allowances. *Energy Economics*, 31(1), 4-15.
- Bierbrauer, M., Trück, S., & Weron, R. (2004). Modeling electricity prices with regime switching models *Computational Science-ICCS 2004* (pp. 859-867): Springer.
- Blunt, M., Fayers, F. J., & Orr, F. M. (1993). Carbon dioxide in enhanced oil recovery. *Energy Conversion and Management*, 34(9), 1197-1204.
- BMUB, A. (2009). *RICHTLINIE 2003/87/EG EMISSIONSHANDELS-RICHTLINIE* Retrieved from http://www.bmub.bund.de/fileadmin/bmu-import/files/pdfs/allgemein/application/pdf/ets_rl_konsolidierte_fassung.pdf.
- BMW. (2015, 20.05.2015). Potenzial von Kavernen vorhersagen. Retrieved from http://forschung-energiespeicher.info/wind-zu-wasserstoff/projektliste/projekt-einzelansicht/74/Potenzial_von_Kavernen_vorhersagen/
- Bock, B., Rhudy, R., Herzog, H., Klett, M., Davison, J., De La Torre Ugarte, D. G., & Simbeck, D. (2003). *Economic evaluation of CO₂ storage and sink enhancement options*. Retrieved from
- Boogert, A., & De Jong, C. (2008). Gas storage valuation using a Monte Carlo method. *The journal of derivatives*, 15(3), 81-98.

- bpb. (2013). Ein Ziel, viele Strategien - Klimapolitik in Deutschland. Retrieved from <http://www.bpb.de/gesellschaft/umwelt/klimawandel/38554/klimapolitik-in-deutschland>
- Budny, C., Madlener, R., & Hilgers, C. (2015). Economic feasibility of pipe storage and underground reservoir storage options for power-to-gas load balancing. *Energy Conversion and Management*, 102, 258-266.
- Bundesregierung. (2015). Energiewende - Maßnahmen im Überblick.
- Carmona, R., & Ludkovski, M. (2010). Valuation of energy storage: An optimal switching approach. *Quantitative Finance*, 10(4), 359-374.
- CCC. (2015). Carbon Budgets and targets. Retrieved from <https://www.theccc.org.uk/tackling-climate-change/reducing-carbon-emissions/carbon-budgets-and-targets/>
- Chen, H., Cong, T. N., Yang, W., Tan, C., Li, Y., & Ding, Y. (2009). Progress in electrical energy storage system: A critical review. *Progress in Natural Science*, 19(3), 291-312.
- Chen, Z., & Forsyth, P. A. (2010). Implications of a regime-switching model on natural gas storage valuation and optimal operation. *Quantitative Finance*, 10(2), 159-176.
- Commission, E. (2015). Allowances and caps. Retrieved from http://ec.europa.eu/clima/policies/ets/cap/index_en.htm
- Connolly, D., Lund, H., Finn, P., Mathiesen, B. V., & Leahy, M. (2011). Practical operation strategies for pumped hydroelectric energy storage (PHES) utilising electricity price arbitrage. *Energy Policy*, 39(7), 4189-4196.
- Crotogino, F., Donadei, S., Bünger, U., Landinger, H., Stolten, D., & Grube, T. (2010). *Large-scale hydrogen underground storage for securing future energy supplies*. Paper presented at the 18th World hydrogen energy conference.
- De Graaf, X. (2013). *Concept development to improve the flexibility of coal-fired plants by supporting the preheating units with solar heat*. (Bachelor of Science), RWTH Aachen.
- Dixit, A. (1989). Entry and exit decisions under uncertainty. *Journal of political Economy*, 620-638.
- Dowideit, M. (2013, 08.10.2013). In der Strombranche ist nichts mehr unmöglich. *Handelsblatt*. Retrieved from <http://www.handelsblatt.com/unternehmen/industrie/kraftwerksbranche-in-aufruhr-in-der-strombranche-ist-nichts-mehr-unmoeglich/8900468.html>
- Drury, E., Denholm, P., & Sioshansi, R. (2011). The value of compressed air energy storage in energy and reserve markets. *Energy*, 36(8), 4959-4973. doi:<http://dx.doi.org/10.1016/j.energy.2011.05.041>
- Eccles, J. K., Pratson, L., Newell, R. G., & Jackson, R. B. (2009). Physical and Economic Potential of Geological CO₂ Storage in Saline Aquifers. *Environmental Science & Technology*, 43(6), 1962-1969. doi:10.1021/es801572e
- Eckroad, S., & Gyuk, I. (2003). EPRI-DOE handbook of energy storage for transmission & distribution applications. *Electric Power Research Institute, Inc.*
- EEX. (2015a). *Day-ahead hourly Phelix spot prices*.
- EEX. (2015b). *EUA secondary market*.
- EEX. (2015c). *NCG area - daily reference spot price - natural gas*.
- EEX. (2015d). *Phelix baseload spot prices*.
- EEX. (2015e). *Phelix peak-load daily contract*.
- EU, E. U. (2009). Directive 2009/29/EC of the European Parliament and of the Council of 23 April 2009 amending Directive 2003/87/EC so as to improve and extend the greenhouse gas emission allowance trading scheme of the Community. *Journal of the European Union*, 5, 2009.
- Eurostat. (2015). Energy Database. Retrieved 20.11.2015, from Eurostat <http://ec.europa.eu/eurostat/web/energy/data/database>

- Eydeland, A., & Wolyniec, K. (2003). *Energy and power risk management: New developments in modeling, pricing, and hedging* (Vol. 206): John Wiley & Sons.
- Fanone, E., Gamba, A., & Prokopczuk, M. (2013). The case of negative day-ahead electricity prices. *Energy Economics*, 35, 22-34.
- Felix, B., Woll, O., & Weber, C. (2013). Gas storage valuation under limited market liquidity: an application in Germany. *The European Journal of Finance*, 19(7-8), 715-733.
- Fischedick, M., Esken, A., Luhmann, H.-J., Schüwer, D., & Supersberger, N. (2007). *Geologische CO₂-Speicherung als klimapolitische Handlungsoption: Technologien, Konzepte, Perspektiven*: Wuppertal Spezial, Wuppertal Institut für Klima, Umwelt und Energie.
- FNB. (2014). FNB Gas - Zahlen und Fakten. Retrieved from <http://www.fnb-gas.de/de/fernleitungsnetze/zahlen-und-fakten/zahlen-und-fakten.html>
- Fraunhofer, I. (2013). Stromgestehungskosten erneuerbare Energien. *Version November*.
- Gal. (2011, 06.06.2011). Kabinett beschließt Atomausstieg bis 2022. *Süddeutsche Zeitung*. Retrieved from <http://www.sueddeutsche.de/politik/gesetzespaket-zur-energie-wende-kabinett-beschliesst-atomausstieg-bis-1.1105474>
- Gas, F. (2015). Marktgebiete. Retrieved from <http://www.fnb-gas.de/de/fernleitungsnetze/marktgebiete/marktgebiete.html>
- Gatzen, C. (2008). *The economics of power storage: Theory and empirical analysis for Central Europe* (Vol. 63): Oldenbourg Industrieverlag.
- Gill, G., & Cowan, G. (2014). Adavale Basin, Queensland Underground Salt Cavern Potential, 11. Retrieved from <http://www.innovativeenergy.com.au/saltcavern/article%20for%20mining%20journal.pdf>
- Gillhaus, A. (2007). *Natural Gas Storage in Salt Caverns - Present Status, Developments and Future Trends in Europe*. Paper presented at the SOLUTION MINING RESEARCH INSTITUTE, Basel, Switzerland.
- Gillhaus, A. (2010). Natural gas storage in salt caverns - Summary of worldwide projects and consequences of varying storage objectives and salt formations *Underground Storage of CO₂ and Energy*: CRC Press.
- Graichen, P., Kleiner, M. M., Litz, P., & Podewils, C. (2015). Die Energiewende im Stromsektor: Stand der Dinge 2014: Rückblick auf die wesentlichen Entwicklungen sowie Ausblick auf 2015 (Analyse), 40. Retrieved from http://www.agoraenergiewende.de/fileadmin/downloads/publikationen/Analysen/Jahresauswertung_2014/Agora_Energiewende_Jahresauswertung_2014_web.pdf
- Hadjipaschalis, I., Poullikkas, A., & Efthimiou, V. (2009). Overview of current and future energy storage technologies for electric power applications. *Renewable and sustainable energy reviews*, 13(6), 1513-1522.
- Hannover, L. (2014). Energie und Geologie (LBEG). Untertage-Gasspeicherung in Deutschland. *ERDÖL ERDGAS KOHLE*, 130(11), 412-423.
- Haubrich, H.-J. (2007). Verbesserte Integration großer Windstrommengen durch Zwischenspeicherung mittels CAES, 143. Retrieved from http://www.bine.info/fileadmin/content/Publikationen/Projekt-Infos/Zusatzinfos/2007-05_Abschlussbericht.pdf
- Holland, A. (2008). Optimization of injection/withdrawal schedules for natural gas storage facilities *Applications and Innovations in Intelligent Systems XV* (pp. 287-300): Springer.
- Huisman, R., Huurman, C., & Mahieu, R. (2007). Hourly electricity prices in day-ahead markets. *Energy Economics*, 29(2), 240-248.
- Institute, E. P. R. (2008). *Compressed air energy storage scoping study for california*. Public Interest Energy Research Program.

- Janczura, J., Trück, S., Weron, R., & Wolff, R. C. (2013). Identifying spikes and seasonal components in electricity spot price data: A guide to robust modeling. *Energy Economics*, 38, 96-110.
- Janczura, J., & Weron, R. (2012). Efficient estimation of Markov regime-switching models: An application to electricity spot prices. *ASIA Advances in Statistical Analysis*, 96(3), 385-407.
- Janczura, J., & Weron, R. (2015). Matlab function to estimate parameters. Retrieved from <https://ideas.repec.org/f/pja256.html#software>
- Keles, D., Genoese, M., Möst, D., & Fichtner, W. (2012). Comparison of extended mean-reversion and time series models for electricity spot price simulation considering negative prices. *Energy Economics*, 34(4), 1012-1032.
- Keles, D., Hartel, R., Möst, D., & Fichtner, W. (2012). Compressed-air energy storage power plant investments under uncertain electricity prices: an evaluation of compressed-air energy storage plants in liberalized energy markets. *Journal of Energy Markets*, 5(1), 53-84.
- Knopf, B. G., Oliver. (2014). A warning from the IPCC: the EU 2030's climate target cannot be based on science alone. Retrieved from energypost website: <http://www.energypost.eu/warning-ipcc-eu-2030s-climate-target-based-science-alone/>
- Koch, N., Fuss, S., Grosjean, G., & Edenhofer, O. (2014). Causes of the EU ETS price drop: Recession, CDM, renewable policies or a bit of everything?—New evidence. *Energy Policy*, 73, 676-685.
- Kosater, P., & Mosler, K. (2006). Can Markov regime-switching models improve power-price forecasts? Evidence from German daily power prices. *Applied Energy*, 83(9), 943-958.
- Kovscek, A. R., & Cakici, M. D. (2005). Geologic storage of carbon dioxide and enhanced oil recovery. II. Cooptimization of storage and recovery. *Energy Conversion and Management*, 46(11-12), 1941-1956. doi:10.1016/j.enconman.2004.09.009
- Kroniger, D., & Madlener, R. (2013). Hydrogen Storage for Wind Parks: A Real Options Evaluation for an Optimal Investment in More Flexibility. *FCN Working Paper No. 3/2013*. Retrieved from
- Krooss, B., Van Bergen, F., Gensterblum, Y., Siemons, N., Pagnier, H., & David, P. (2002). High-pressure methane and carbon dioxide adsorption on dry and moisture-equilibrated Pennsylvanian coals. *International Journal of Coal Geology*, 51(2), 69-92.
- Lai, G., Margot, F., & Secomandi, N. (2010). An approximate dynamic programming approach to benchmark practice-based heuristics for natural gas storage valuation. *Operations research*, 58(3), 564-582.
- Liebl, D. (2013). Modeling and forecasting electricity spot prices: A functional data perspective. *The Annals of Applied Statistics*, 7(3), 1562-1592.
- Loisel, R., Mercier, A., Gatzert, C., Elms, N., & Petric, H. (2010). Valuation framework for large scale electricity storage in a case with wind curtailment. *Energy Policy*, 38(11), 7323-7337. doi:<http://dx.doi.org/10.1016/j.enpol.2010.08.007>
- Longstaff, F. A., & Schwartz, E. S. (2001). Valuing American options by simulation: a simple least-squares approach. *Review of Financial studies*, 14(1), 113-147.
- Lukawski, M. Z., Anderson, B. J., Augustine, C., Capuano Jr, L. E., Beckers, K. F., Livesay, B., & Tester, J. W. (2014). Cost analysis of oil, gas, and geothermal well drilling. *Journal of Petroleum Science and Engineering*, 118, 1-14. doi:<http://dx.doi.org/10.1016/j.petrol.2014.03.012>
- Lund, H., Salgi, G., Elmegaard, B., & Andersen, A. N. (2009). Optimal operation strategies of compressed air energy storage (CAES) on electricity spot markets with fluctuating prices. *Applied thermal engineering*, 29(5), 799-806.

- Maragos, S., & Ronn, E. (2002). Valuation of the operational flexibility of natural gas storage reservoirs. *Real Options and Energy Management Using Options Methodology to Enhance Capital Budgeting Decisions*, 431-456.
- McCoy, S. T. (2008). *The economics of carbon dioxide transport by pipeline and storage in saline aquifers and oil reservoirs*: ProQuest.
- McCoy, S. T., & Rubin, E. S. (2009). Variability and uncertainty in the cost of saline formation storage. *Energy Procedia*, 1(1), 4151-4158.
doi:10.1016/j.egypro.2009.02.224
- Middleton, R. S., & Bielicki, J. M. (2009). A scalable infrastructure model for carbon capture and storage: SimCCS. *Energy Policy*, 37(3), 1052-1060.
doi:10.1016/j.enpol.2008.09.049
- Muche, T. (2009). A real option-based simulation model to evaluate investments in pump storage plants. *Energy Policy*, 37(11), 4851-4862. doi:10.1016/j.enpol.2009.06.041
- Nadarajah, S., Margot, F., & Secomandi, N. (2014). Relaxations of approximate linear programs for the real option management of commodity storage. *Available at SSRN 2497666*.
- NEP, N. S. (2013). Zweiter Entwurf der Übertragungsnetzbetreiber. Retrieved from <http://www.netzentwicklungsplan.de/content/netzentwicklungsplan-2013-zweiter-entwurf>
- Nowotarski, J., Tomczyk, J., & Weron, R. (2013). Robust estimation and forecasting of the long-term seasonal component of electricity spot prices. *Energy Economics*, 39, 13-27.
- Oldenburg, C. M. (2003). Carbon dioxide as cushion gas for natural gas storage. *Energy & Fuels*, 17(1), 240-246.
- Ozarslan, A. (2012). Large-scale hydrogen energy storage in salt caverns. *International Journal of Hydrogen Energy*, 37(19), 14265-14277.
doi:10.1016/j.ijhydene.2012.07.111
- Petroleum, B. (2015). BP Statistical Review of World Energy 2015. Retrieved from <http://www.bp.com/en/global/corporate/energy-economics/statistical-review-of-world-energy.html>
- Pilipovic, D. (2007). *Energy Risk: Valuing and Managing Energy Derivatives: Valuing and Managing Energy Derivatives*: McGraw Hill Professional.
- Prognos. (2013). *Entwicklung von Stromproduktionskosten - Die Rolle von Freiflächen-Solkraftwerken in der Energiewende, Studie im Auftrag der BELECTRIC Solarkraftwerke GmbH*. Retrieved from Berlin:
- Quandl. (2015). *ECX EUA Futures - Front month continuous contract*. Retrieved from: https://www.quandl.com/data/CHRIS/ICE_C1
- Raju, M., & Kumar Khaitan, S. (2012). Modeling and simulation of compressed air storage in caverns: A case study of the Huntorf plant. *Applied Energy*, 89(1), 474-481.
doi:10.1016/j.apenergy.2011.08.019
- Rapoza, K. (2015, 05.05.2015). The U.S. Cannot Compete With Russia In Europe's Natural Gas Market. *Forbes*.
- Reuters, T. (2015a). *API2 Coal Index +exchange rate USD/EUR*.
- Reuters, T. (2015b). *EGIX NCG monthly continous gas price index*.
- Reuters, T. (2015c). *Phelix Base - four day moving average*.
- Ross, S. A., Westerfield, R., & Jordan, B. D. (2008). *Fundamentals of corporate finance*: Tata McGraw-Hill Education.
- Saur, G., & Ainscough, C. (2011). US Geographic Analysis of the Cost of Hydrogen from Electrolysis. *Contract*, 303, 275-3000.
- Schröder, D. (2014, 30.04.2014). Gas-Speicher vor dem Abschluss. *az-online*.
- Schroeter, S. (2014, 21.10.2014). Dritte Kaverne für den Erdgasspeicher Katharina. *Stefanschroeter.com*.
- Schürmeyer, J. (2013, 16.05.2013). Gashahn in Jemgum *NWZ online*.

- Schwartz, E. S. (1997). The stochastic behavior of commodity prices: Implications for valuation and hedging. *The Journal of Finance*, 52(3), 923-973.
- Seifert, J., & Uhrig-Homburg, M. (2007). Modelling jumps in electricity prices: theory and empirical evidence. *Review of Derivatives Research*, 10(1), 59-85.
- Sioshansi, R., Denholm, P., & Jenkin, T. (2011). A comparative analysis of the value of pure and hybrid electricity storage. *Energy Economics*, 33(1), 56-66.
doi:<http://dx.doi.org/10.1016/j.eneco.2010.06.004>
- Sioshansi, R., Denholm, P., Jenkin, T., & Weiss, J. (2009). Estimating the value of electricity storage in PJM: Arbitrage and some welfare effects. *Energy Economics*, 31(2), 269-277. doi:<http://dx.doi.org/10.1016/j.eneco.2008.10.005>
- Sørensen, B. (2007). *Geological hydrogen storage*. Paper presented at the Proc. World Hydrogen Technologies Conf.
- Stronzik, M., Neumann, A., & Rammerstorfer, M. (2008). *Wettbewerb im Markt für Erdgasspeicher: WIK*.
- Struck, D. (1993). *Gebirgsmechanische Untersuchungen zur Bestimmung des Maximaldrucks von Salzkavernen* (Vol. Heft 15). Hannover: Rokahr, R. B.
- Taylor, J., Alderson, J., Kalyanam, K., Lyle, A., & Phillips, L. (1986). Technical and economic assessment of methods for the storage of large quantities of hydrogen. *International Journal of Hydrogen Energy*, 11(1), 5-22.
- Thompson, M. (2012). *Natural gas storage valuation, optimization, market and credit risk management*. Retrieved from
- Thompson, M., Davison, M., & Rasmussen, H. (2009). Natural gas storage valuation and optimization: A real options application. *Naval Research Logistics (NRL)*, 56(3), 226-238.
- Trianel. (2010). Trianel Gasspeicher Epe verdoppelt Kapazität [Press release]. Retrieved from <http://www.presseportal.de/pm/67884/1633048>
- van der Zwaan, B., & Smekens, K. (2007). CO2 Capture and Storage with Leakage in an Energy-Climate Model. *Environmental Modeling & Assessment*, 14(2), 135-148.
doi:10.1007/s10666-007-9125-3
- Vassiliadis, M. (2015). Emissionshandel soll repariert werden – aber erst in ein paar Jahren. Retrieved from <http://www.nachhaltigkeitsrat.de/index.php?id=8901>
- Weron, R. (2007). *Modeling and forecasting electricity loads and prices: a statistical approach* (Vol. 403): John Wiley & Sons.
- Weron, R. (2014). Electricity price forecasting: A review of the state-of-the-art with a look into the future. *International Journal of Forecasting*, 30(4), 1030-1081.
- Weron, R., Bierbrauer, M., & Trück, S. (2004). Modeling electricity prices: jump diffusion and regime switching. *Physica A: Statistical Mechanics and its Applications*, 336(1), 39-48.
- Weston, T., & Ronn, E. (2002). Applying stochastic dynamic programming to the valuation of gas storage and generation assets. *Real Options and Energy Management Using Options Methodology to Enhance Capital Budgeting Decisions*, 183-216.
- Zander-Schiebenhöfer, D., Donadei, S., Horvath, P.-L., Zapf, D., Staudtmeister, K., & Rokahr, R. B. (2015). Bestimmung des Speicherpotenzials Erneuerbarer Energien in den Salzstrukturen Norddeutschlands: Projekt InSpEE. *ERDÖL ERDGAS KOHLE*, 131(01/2015), 289-293.

Appendix

The detailed MATLAB code, all used data sets and the entire bibliography are available upon request.

A1 Electricity price simulation

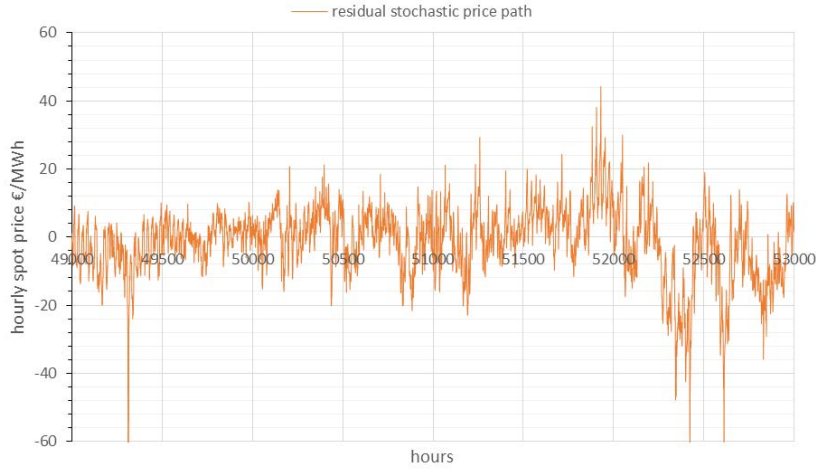


Figure 33: Residual stochastic price path after removal of the daily, weekly, seasonal and long-term cycles.

Following paragraph describes the electricity price simulation process:

1. Perform a Fourier Fit on the dataset of daily spot prices to estimate the long-term cycle. Use the non-linear least squares method with a filter to decrease the weight of outliers (Bisquare Robust in Matlab). The resulting equation has the following form:

$$P_{D-ltc} = a_0 + a_1 * \cos(x * w) + b_1 * \sin(x * w) \quad (22)$$

2. Convert daily data to hourly data.

$$P_{H-ltc} = a_0 + a_1 * \cos\left(\frac{x}{24} * w\right) + b_1 * \sin\left(\frac{x}{24} * w\right) \quad (23)$$

3. Remove long-term cycle (ltc) from historical hourly spot price data.

$$P_{spot-ltc} = P_{spothourly} - P_{H-ltc} \quad (24)$$

4. Deseasonalize $P_{spot-ltc}$ using the JW-algorithm²⁶. The algorithm returns three components: the deseasonalized price path $P_{des1-ltc}$, a long-term seasonal price path P_{lts1} and a short-term seasonal price path P_{sts1} .

5. Calculate mean μ_{des} and standard error σ_{des} of deseasonalized prices $P_{des1-ltc}$. Start outlier correction by replacing all prices exceeding the interval $[\mu_{des} \pm 3\sigma_{des}]$ with the mean price μ_{des} .

6. Rebuild dataset using the deseasonalization components and the outlier corrected residual price:

$$P_{corr-rebuild} = P_{lts} + P_{sts} + P_{corr-des1-ltc} \quad (25)$$

7. Run the JW-algorithm to deseasonalize. See Figure 8 for results.

8. Remove short-term cycle:

$$P_{corr-stc2} = P_{spot-ltc} - P_{stc2} \quad (26)$$

9. Perform a Fourier Fit based on $P_{corr-stc2}$ to estimate the seasonal cycle. Use the same approach as in 1. The resulting equation has the following form:

²⁶ JW-algorithm presented in Janczura and Weron (2012), Janczura et al. (2013) and Janczura and Weron (2015)

$$P_{ssc} = a_0 + a_1 * \cos(x * w) + b_1 * \sin(x * w) \quad (27)$$

10. Construct residual price curve. Graphical results are shown in figure 33.

$$P_{res-stoch} = P_{corr-stc2} - P_{ssc} \quad (28)$$

11. To evaluate the long-term value of the storage, the simulation time is 25 years with 500 price paths.

12. Run the JW-algorithm - MRS_est to estimate parameters of Markov regime-switching model. Use the exponential model, since it has the best fit on data.

13. Run the simulation algorithm MRS_sim to generate values for base, spike and drop regime for the upcoming 25 years.

14. Add all components to P_{sim} .

$$P_{sim} = P_{stoch} + P_{ssc} + P_{stc2} + P_{H-ltc} \quad (29)$$

A2 Gas price simulation

Following paragraph describes the gas price simulation process:

1. Perform a Fourier Fit on the dataset of the daily spot prices to estimate the long-term cycle. Use the non-linear least squares method with a filter to decrease the weight of outliers (Bisquare Robust in Matlab). The resulting equation has the following form:

$$P_{G-ltc} = a_0 + a_1 * \cos(x * w) + b_1 * \sin(x * w) \quad (30)$$

The results and coefficients of this regression (PG-ltc) are shown in figure 12 and table 4.

2. Remove long-term cycle (ltc) from historical hourly spot price data.

$$P_{G-spot-ltc} = P_{G-spot} - P_{G-ltc} \quad (31)$$

3. Deseasonalize $P_{G-spot-ltc}$ using the algorithm presented in (Janczura & Weron, 2015). Algorithm returns three components: the deseasonalized price path $P_{G-des1-ltc}$, a long-term seasonal price path P_{G-ltc1} , and a short-term seasonal price path P_{G-stc1} .

4. Calculate mean μ_{des} and standard error σ_{des} of deseasonalized prices $P_{G-des1-ltc}$. Start outlier correction by replacing all prices exceeding the interval $[\mu_{des} \pm 3\sigma_{des}]$ with the mean price μ_{des} .

5. Rebuild dataset using the deseasonalization components and the outlier-corrected residual price:

$$P_{G-corr-rebuild} = P_{G-ltc1} + P_{G-stc1} + P_{G-corr-des1-ltc} \quad (32)$$

6. Run the JW-algorithm again to deseasonalize (see Figure 13 for results).

7. Remove short-term cycle:

$$P_{G-corr-stc2} = P_{spot-ltc} - P_{G-stc2} \quad (33)$$

8. Perform a Fourier Fit based on $P_{G-corr-stc2}$ to estimate the seasonal cycle. Use the same properties as in 2., but now perform a double Fourier Fit. The resulting equation has the following form:

$$P_{G-ssc} = a_0 + a_1 * \cos(x * w) + b_1 * \sin(x * w) + a_2 * \cos(x * w) + b_2 * \sin(x * w) \quad (34)$$

Results and coefficients of this regression can be seen in figure 12.

$$9. \quad P_{G-res-stoch} = P_{G-corr-stc2} - P_{G-ssc} \quad (35)$$

Graphical results are shown in figure 34

11. To evaluate the long-term value of the storage, the simulation time is 25 years with 500 price paths.
12. Run the JW-algorithm - MRS_est to estimate parameters of Markov regime-switching model. Use the logarithmic model, since it has the best fit on data.
13. Run the simulation algorithm MRS_sim to generate values for base and spike regime for the upcoming 25 years.

$$14. \quad P_{G-sim} = P_{G-stoch} + P_{G-ssc} + P_{G-stc2} + P_{G-ltc} \quad (36)$$

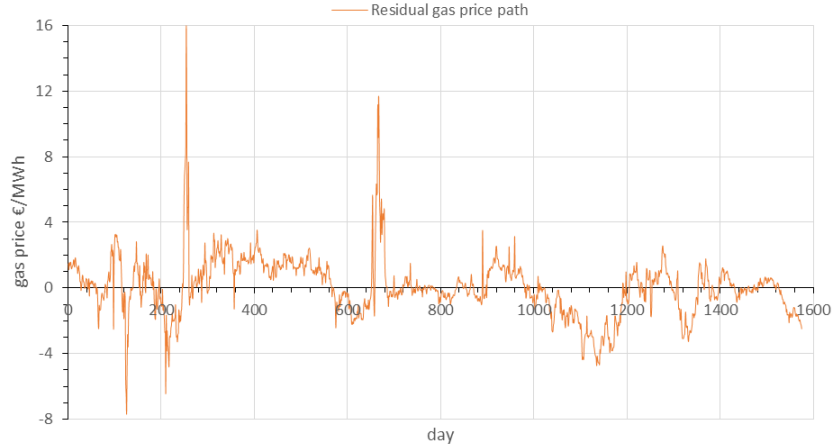


Figure 34: Residual gas price path after removal of all long-term, seasonal and short-term patterns.

A3 CO2 price simulation

Following paragraph describes the carbon price simulation process:

1. Estimate parameters of root / power function:

$$P_{CO2-trend1} = a \cdot x^b \quad (37)$$

Results are shown in Table 6 and figure 15.

$$2. \quad P_{CO2-res1} = P_{CO2-spot} - P_{CO2-trend1} \quad (38)$$

3. Estimate parameters of exponential fit on residual data:

$$P_{CO2-trend2} = c * e^{d*x} \quad (39)$$

Results are shown in Table 6 and figure 15.

$$4. \quad P_{CO2-res} = P_{CO2-res1} - P_{CO2-trend2} \quad (40)$$

5. Estimate parameters of Markov base regime, see digital appendix for exact approach
6. To evaluate the long-term value of the storage, the simulation time is 25 years with 500 price paths. Simulate Markov base regime by means of an Ornstein-Uhlenbeck process.

$$P_{CO2-sim} = P_{CO2-stoch} + P_{CO2-trend} \quad (41)$$

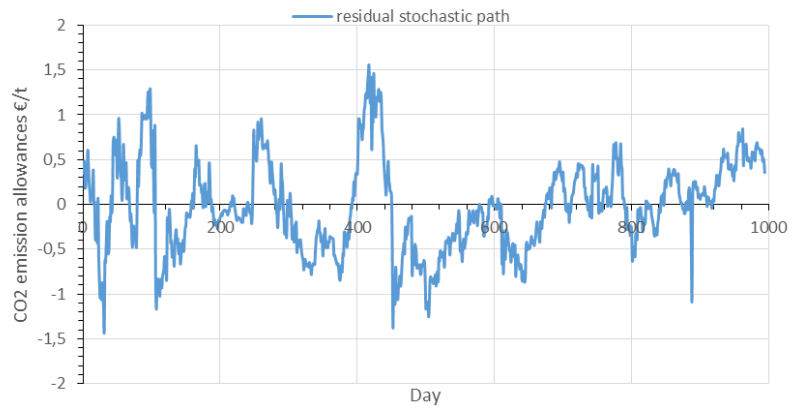


Figure 35: EUA residual stochastic path after removal of combined trend

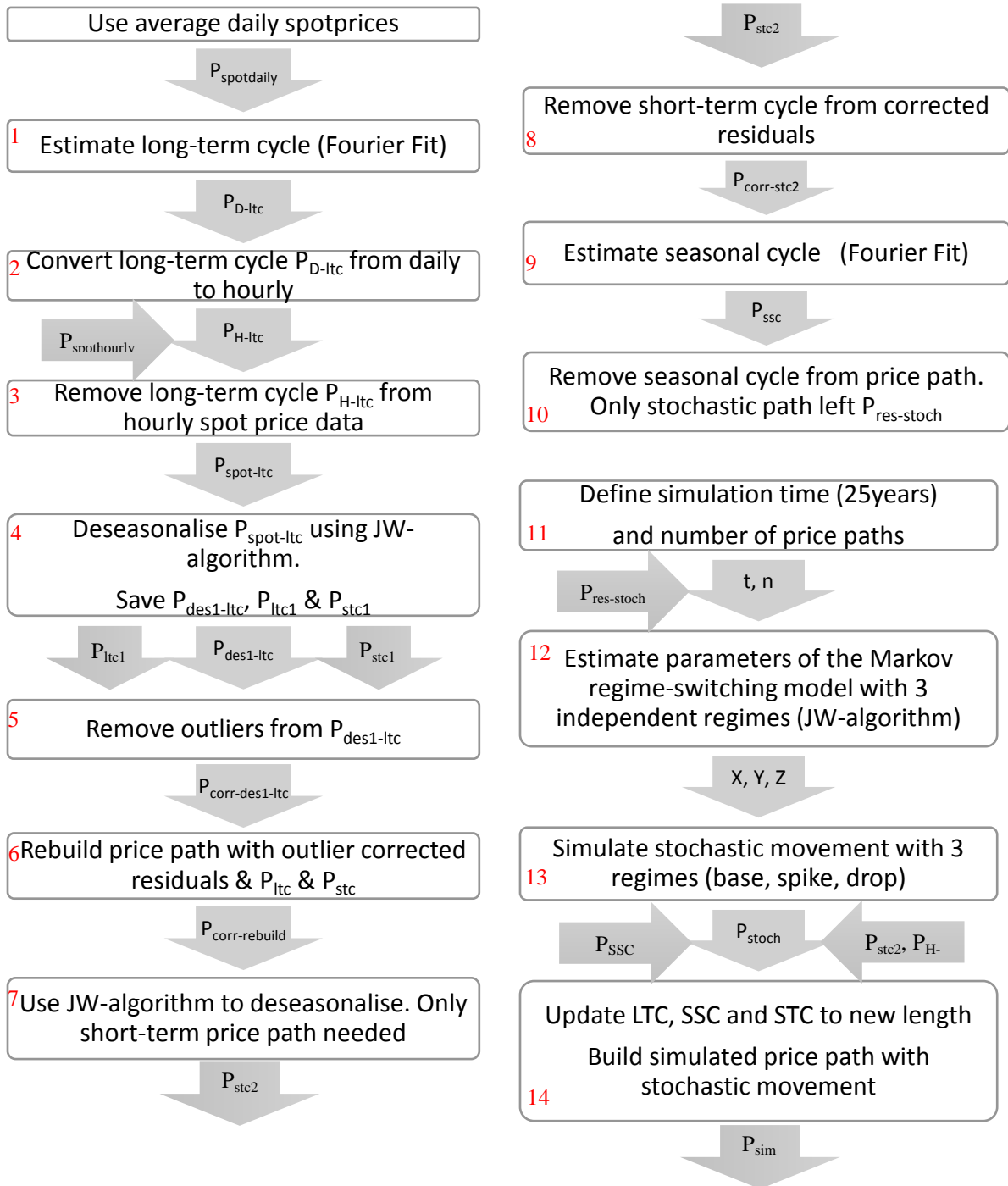


Figure 36: Price modelling flow chart

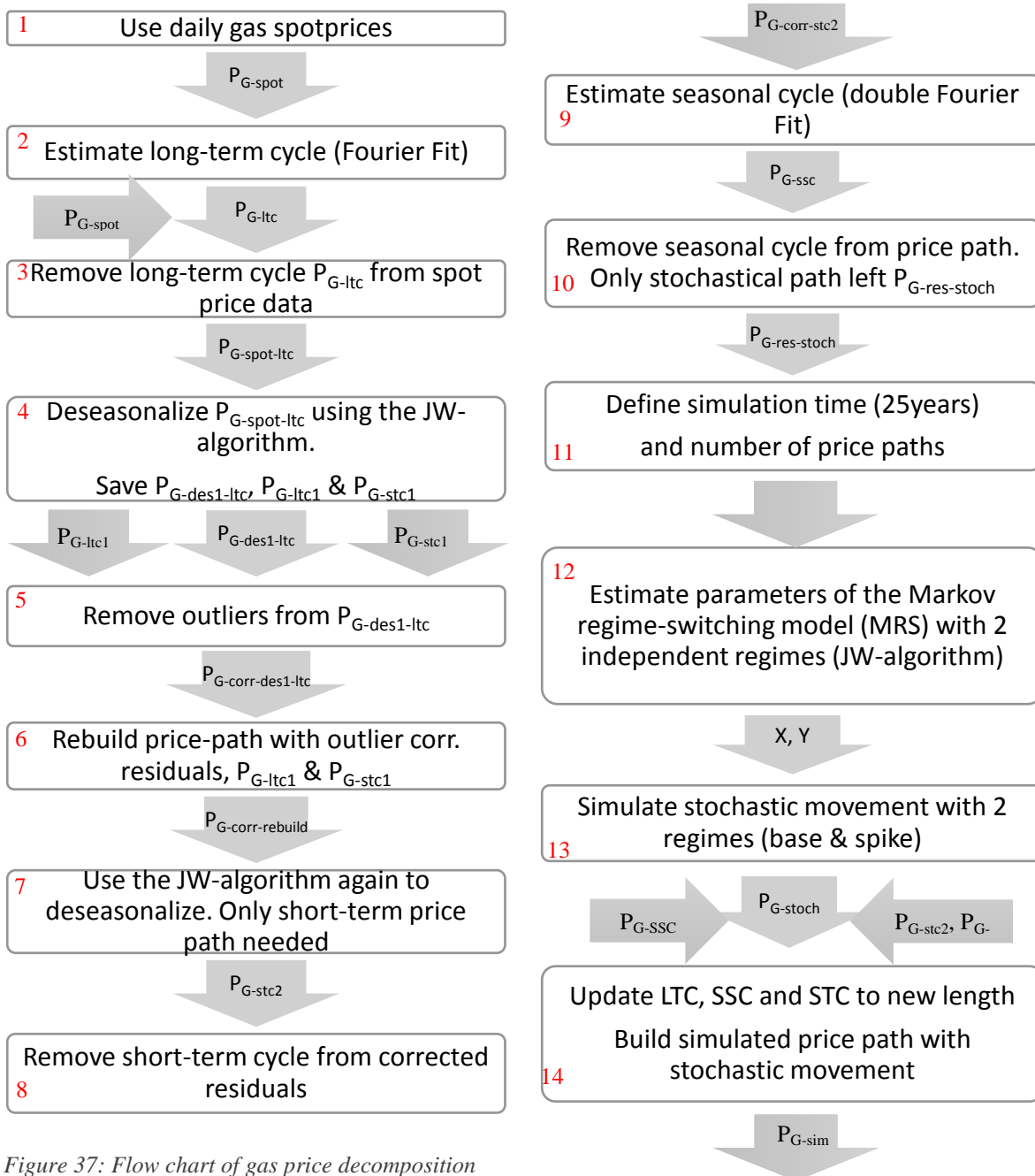


Figure 37: Flow chart of gas price decomposition

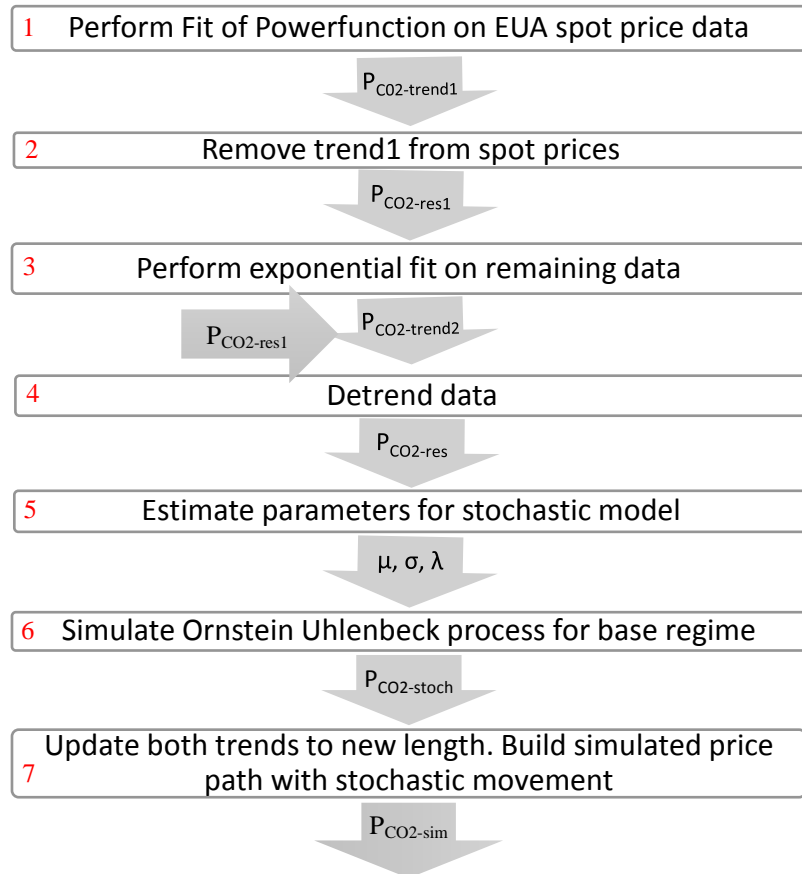


Figure 38: Flowchart of CO₂- price decomposition